Bright Hydrogen-Light Source due to a Resonant Energy Transfer with Strontium and Argon Ions

Randell L. Mills
Mark Nansteel
Paresh Ray

BlackLight Power, Inc.
493 Old Trenton Road
Cranbury, NJ 08512

Abstract

A plasma called an rt-plasma formed with a low field (1V/cm), at low temperatures (e.g. $\approx 10^3\ K$), from atomic hydrogen generated at a tungsten filament and strontium which was vaporized by heating the metal. Strong VUV emission was observed that increased with the addition of argon, but not when sodium, magnesium, or barium replaced strontium or with hydrogen, argon, or strontium alone. Characteristic emission was observed which supported a resonance-energy-transfer mechanism. Significant Balmer α line broadening corresponding to an average hydrogen atom temperature of 14, 24 eV, and 23-45 eV was observed for strontium and argon-strontium rt-plasmas and discharges of strontium-hydrogen, helium-hydrogen, argon-hydrogen, strontium-helium-hydrogen, and strontium-argon-hydrogen, respectively, compared to $\approx 3\ eV$ for pure hydrogen, krypton-hydrogen, xenon-hydrogen, and magnesium-hydrogen. To achieve that same optically measured light output power, hydrogen-sodium, hydrogen-magnesium, and hydrogen-barium mixtures required 4000, 7000, and 6500 times the power of the hydrogen-strontium mixture, respectively, and the addition of argon increased these ratios by a factor of about two. A glow discharge plasma formed for hydrogen-strontium mixtures at an extremely low voltage of about 2 V compared to 250 V for hydrogen alone and sodium-hydrogen mixtures, and 140-150 V for hydrogen-magnesium and hydrogen-barium mixtures.

Key Words: resonance transfer plasma, hydrogen catalysts, VUV emission, plasma light source

I. INTRODUCTION

Suitable hydrogen plasma light sources and spectrometers have been developed which permit observations in the vacuum ultraviolet (VUV). Developed sources that provide a suitable intensity are high voltage glow discharges, synchrotron devices, inductively coupled plasma generators [1], and magnetically confined plasmas. Glow discharge devices have been developed over decades as light sources, ionization sources for mass spectroscopy, excitation sources for optical spectroscopy, and sources of ions for surface etching and chemistry [2-4]. A Grimm-type glow discharge is a well established excitation source for the analysis of conducting solid samples by optical emission spectroscopy [5-7]. Despite extensive performance characterizations, data was lacking on the plasma parameters of these devices. M. Kuraica and N. Konjevic [8] and Videnovic et al. [9] have characterized these plasmas by determining the excited hydrogen atom concentrations and energies from measurements of the line broadening of the 656.3 nm Balmer α line. The data was analyzed in terms of external Stark and Doppler effects wherein acceleration of charges such as H^+, H_2^+, and H_3^+ in the high fields (e. g. over $10\,kV/cm$) which were present in the cathode fall region was used to explain the Doppler component.

More recently, microhollow glow discharges have been spectroscopically studied as candidates for the development of an intense monochromatic VUV light source (e.g. Lyman α) for short wavelength lithograph for production of the next generation of integrated circuits. A neon-hydrogen microhollow cathode glow discharge has been proposed as a source of predominantly Lyman α radiation. Kurunczi, Shah, and Becker [10] observed intense emission of Lyman α and Lyman β radiation at 121.6 nm and 102.5 nm, respectively, from microhollow cathode discharges in high-pressure Ne (740 Torr) with the addition of a small amount of hydrogen (up to 3 Torr). With essentially no molecular emission observed, Kurunczi et al. attributed the anomalous Lyman α emission to the near-resonant energy transfer between the Ne_2^* excimer and H_2 which leads to formation of $H(n=2)$ atoms, and attributed the Lyman β emission to the near-resonant energy transfer between excited Ne^* atoms (or vibrationally excited neon excimer molecules) and H_2

which leads to formation of $H(n=3)$ atoms. Despite the emission characterization of this source, data is lacking about plasma parameters.

For analyses of solids, direct current (dc) glow discharge sources have been successfully complemented by radio-frequency (rf) discharges [11]. The use of dc discharges is limited to metals; whereas, rf discharges are applicable to non-conducting materials. Other developed sources that provide a usefully intense plasma are synchrotron devices, inductively coupled plasma generators [12], and magnetically confined plasmas. Plasma characterization data on these sources is also limited.

A new plasma source has been developed that operates by incandescently heating a hydrogen dissociator and a catalyst to provide atomic hydrogen and gaseous catalyst, respectively, such that the catalyst reacts with the atomic hydrogen to produce a plasma called a resonance transfer, (rt)-plasma. The plasma forms by a resonance transfer mechanism involving the species providing a net enthalpy of a multiple of $27.2\,eV$ and atomic hydrogen. It was extraordinary, that intense VUV emission was observed [13-20] at low temperatures (e.g. $\approx 10^3\,K$) from atomic hydrogen and certain atomized elements or certain gaseous ions which singly or multiply ionize at integer multiples of the potential energy of atomic hydrogen, $27.2\,eV$ that comprise catalysts. The only pure elements that were observed to emit VUV were those wherein the ionization of t electrons from an atom to a continuum energy level is such that the sum of the ionization energies of the t electrons is approximately $m \cdot 27.2\,eV$ where t and m are each an integer (e.g. K, Cs, Sr, Sr^+, and Rb^+ each ionize at integer multiples of the potential energy of atomic hydrogen and caused emission; whereas, the chemically similar atoms, Na, Mg, and Ba, do not ionize at integer multiples of the potential energy of atomic hydrogen and caused no emission). The theory has been given previously [16, 20-21].

He^+ ionizes at $54.417\,eV$ which is $2 \cdot 27.2\,eV$. While the ionization energy of Ar^+ to Ar^{2+} is $27.6\,eV$ [22] and the ionization of Sr^+ to Sr^{3+} has a net enthalpy of reaction of $53.92\,eV$ [22], an electric field may adjust the energy of ionizing Ar^+ to Ar^{2+} and Sr^+ to Sr^{3+} to match the energy of $27.2\,eV$ and $2 \cdot 27.2\,eV$, respectively. It was reported previously that characteristic emission was observed from a continuum state of Ar^{2+} at $45.6\,nm$ without the typical Rydberg series of Ar I and Ar II lines which

confirmed the resonant nonradiative energy transfer of $27.2\,eV$ from atomic hydrogen to Ar^+ [14]. Predicted emission lines were observed from helium-hydrogen [20-21] as well as strontium-argon-hydrogen plasmas [14] that supported the rt-plasma mechanism.

To further characterize strontium and argon-strontium rt-plasmas and the catalyst mechanism, plasma formation studies, VUV spectroscopy, broadening of the Balmer α line, and optical power balance measurements were performed relative to mixtures of hydrogen and chemically similar controls that do not have electron ionization energies which are a multiple of $27.2\,eV$. Four different light sources were used to form and characterize the rt-plasmas under a range of plasma conditions.

II. EXPERIMENTAL

A. VUV spectroscopy

Due to the short wavelength of this radiation, "transparent" optics do not exist for VUV spectroscopy. Therefore, a windowless arrangement was used wherein the source was connected to the same vacuum vessel as the grating and detectors of the VUV spectrometer. Windowless VUV spectroscopy was performed with a vacuum ultraviolet spectrometer that was mated with the cell. Differential pumping permitted a high pressure in the cell as compared to that in the spectrometer. This was achieved by pumping on the cell outlet and pumping on the grating side of the collimator that served as a pin-hole inlet to the optics. The cell was operated under gas flow conditions while maintaining a constant gas pressure in the cell. The gas pressure inside the cell was maintained at about 300 mtorr with a hydrogen flow rate of 5.5 sccm controlled by a 0-20 sccm range mass flow controller with a readout. The argon-hydrogen gas mixture which produced the maximum VUV emission was determined by adjusting the flow rate of hydrogen and argon with two mass flow controllers such that the total was 5.5 sccm.

The experimental set up of a Type I light source shown in Figure 1 comprised a quartz cell which was 500 mm in length and 50 mm in diameter. A Pyrex cap sealed to the quartz cell with a Viton O ring and a C-clamp incorporated ports for gas inlet, outlet, and photon detection. A

tungsten filament (0.508 mm in diameter and 800 cm in length, total resistance ~2.5 ohm) heater and hydrogen dissociator were in the quartz tube as well as a cylindrical titanium screen (300 mm long and 40 mm in diameter) that served as a second hydrogen dissociator in the case of the hydrogen gas experiments. A new dissociator was used for each hydrogen gas experiment. The filament was coiled on a grooved ceramic tube support to maintain its shape when heated. The return lead passed through the inside of the ceramic tube. The titanium screen was electrically floated. Power was applied to the filament by a DC power supply which was controlled by a constant power controller. The temperature of the tungsten filament was estimated to be in the range 1100 to 1500°C. The external cell wall temperature was about 700°C. The entire quartz cell was enclosed in an Alumina insulation package. Several K-type thermocouples were located in the insulation. The thermocouples were monitored with a multichannel computer data acquisition system.

In the present study, the light emission phenomena was studied for 1.) hydrogen, argon, neon, and helium alone; 2.) sodium, magnesium, barium, and strontium metals alone; 3.) sodium, magnesium, barium, and strontium with hydrogen; and 4.) sodium, magnesium, barium, and strontium with an argon-hydrogen mixture (97/3%). 1 g of the pure metal (Alfa Aesar 99.95%) of sodium, magnesium, barium, or strontium was placed in the center of the cell under one atmosphere of dry argon in a glovebox. The cell was sealed, removed from the glovebox, and connected to an VUV spectrometer. Each metal was vaporized by the filament heater. The power applied to the filament was 300 W in the case of strontium and up to 600 watts in the case of magnesium, barium, or sodium metal. The voltage across the filament was about 55 V and the current was about 5.5 ampere at 300 watts. For each control, sodium, magnesium, or barium metal, the cell temperature was increased to the maximum permissible with the power supply.

The light emission was introduced to a VUV spectrometer for spectral measurement. The spectrometer was a 0.2 meter monochromator (Seya-Namioka mounting) equipped with a 1200 lines/mm holographic grating with a platinum coating. The wavelength region covered by the monochromator was $30-560\,nm$. A channel

electron multiplier (CEM) was used to detect the VUV light. The wavelength resolution was about 0.2 *nm* (FWHM) with an entrance and exit slit width of 40 μm. The vacuum inside the monochromator was maintained below $5X10^{-4}$ torr by a turbo pump. The VUV spectrum (40 – 160 *nm*) of the cell emission with strontium present was recorded at about the point of the maximum Lyman α emission.

The UV/VIS spectrum (40 – 560 *nm*) of the cell emission with hydrogen alone was recorded with a photomultiplier tube (PMT) and a sodium salicylate scintillator. The PMT used had a spectral response in the range of 185 – 680 *nm* with a peak efficiency at about 400 *nm*. The scan interval was 0.2 *nm*. The inlet and outlet slit were 40 μm with a corresponding wavelength resolution of 0.2 *nm*.

Standard vacuum ultraviolet emission spectra of hydrogen and argon were obtained with a Type II light source comprising a microwave plasma system and an VUV spectrometer shown in Figure 2. The microwave generator was a Opthos model MPG-4M generator (Frequency: 2450 MHz). The output power was set at about 85 W. Hydrogen or argon was flowed through a quartz tube (1.25 cm ID, 20 cm long) at 500 mtorr. The tube was fitted with an Opthos coaxial microwave cavity (Evenson cavity), and was directly connected to the collimator port of an VUV spectrometer. In the case of hydrogen, the VUV spectrometer was the McPherson model 302 (Seya-Namioka type) normal incidence monochromator. The monochromator slits were $100X100\ \mu m$. A sodium salicylate converter was used, and the emission was detected with a photomultiplier tube detector (Hamamatsu R1527P). To achieve higher sensitivity at the shorter VUV wavelengths, the argon plasma light emission was recorded with a McPherson 4° grazing incidence VUV spectrometer (Model 248/310G) equipped with a grating having 600 G/mm with a radius of curvature of $\approx 1\ m$. The angle of incidence was 87°. The wavelength region covered by the monochromator was 1 – 65 *nm*. The wavelength resolution was about 0.1 *nm* (FWHM) with an entrance and exit slit width of 50 μm. A channel electron multiplier (CEM) was used to detect the VUV light. The vacuum inside the monochromator was maintained below $5X10^{-4}$ torr by a turbo pump.

B. Balmer line broadening recorded by high resolution visible

The method of Videnovic et al. [9] was used to calculate the energetic hydrogen atom densities and energies from the width of the 656.3 nm Balmer α line emitted from glow discharge and microwave plasmas. The full half-width $\Delta\lambda_G$ of each Gaussian results from the Doppler ($\Delta\lambda_D$) and instrumental ($\Delta\lambda_I$) half-widths:

$$\Delta\lambda_G = \sqrt{\Delta\lambda_D^2 + \Delta\lambda_I^2} \quad (1)$$

$\Delta\lambda_I$ in our experiments was $0.025\,nm$. The temperature was calculated from the Doppler half-width using the formula:

$$\Delta\lambda_D = 7.16\,X\,10^{-7}\lambda_0\left(\frac{T}{\mu}\right)^{1/2} \quad (nm) \quad (2)$$

where λ_0 is the line wavelength in nm, T is the temperature in K ($1\,eV = 11{,}605\,K$), and μ is the molecular weight (=1 for hydrogen). In each case, the average Doppler half-width that was not appreciably changed with pressure varied by ±4% corresponding to an error in the energy of ±4%. The corresponding number densities for noble gas-hydrogen mixtures varied by ±8% depending on the pressure.

The width of the 656.3 nm Balmer α line was recorded on light emitted from a hydrogen glow discharge performed according to methods reported previously [23] and maintained in the cylindrical stainless steel gas cell comprising a Type III light source shown in Figure 3 that served as a control for measurements recorded on light emitted from rt-plasmas of hydrogen with strontium or strontium with an argon-hydrogen mixture (97/3%) maintained in Type I cells. The inorganic test materials were coated on a titanium screen dissociator by the method of wet impregnation. The screen was coated by dipping it in a 0.6 M $SrCO_3$/10% H_2O_2, and the crystalline material was dried on the surface by heating for 12 hours in a drying oven at 130 °C.

The plasma emission from the hydrogen glow discharge (Type III light source) and each rt-plasma maintained in the filament heated cell (Type I light source) was fiber-optically coupled through a 220F matching fiber adapter positioned 2 cm from the sapphire window or cell wall, respectively, to a high resolution visible spectrometer with a resolution of $\pm 0.006\,nm$ over the spectral range $190\text{-}860\,nm$. The spectrometer was a Jobin Yvon Horiba 1250 M with 2400 groves/mm

ion-etched holographic diffraction grating. The entrance and exit slits were set to 20 μm. The spectrometer was scanned between 655.5-657 nm using a 0.01 nm step size. The signal was recorded by a PMT with a stand alone high voltage power supply (950 V) and an acquisition controller. The data was obtained in a single accumulation with a 1 second integration time. The high resolution visible spectrum 400-410 nm was also recorded on the strontium plasma to record Sr and Sr^+ lines.

In addition, the width of the 656.3 nm Balmer α line emitted from gas discharge plasmas having atomized hydrogen from pure hydrogen alone, hydrogen with magnesium or strontium, a mixture of 10% hydrogen and helium, argon, krypton, or xenon, a mixture of 10% hydrogen and helium or argon with strontium, and argon with strontium was measured with a high resolution visible spectrometer with a resolution of $\pm 0.025\ nm$ over the spectral range 190-860 nm. The plasmas were maintained in a Type III light source.

The 304-stainless steel cylindrical cell was 9.21 cm in diameter and 14.5 cm in height. The base of the cell contained a welded-in stainless steel thermocouple well (1 cm OD) which housed a thermocouple probe in the cell interior approximately 2 cm from the discharge and 2 cm from the cell axis. At the middle height of the cell wall was a welded-flush stainless steel tube (0.95 cm diameter) which was connected to a flexible stainless steel tube (100 cm in length) that served as a vacuum line from the cell and the line to supply the test gas. The top end of the cell was welded to a high vacuum 11.75 cm diameter conflat flange. A silver plated copper gasket was placed between a mating flange and the cell flange. The two flanges were clamped together with 10 circumferential bolts. The mating flange contained two penetrations comprising 1.) a stainless steel thermocouple well (1 cm OD) also housing a thermocouple probe in the cell interior approximately 2 cm from the discharge and 2 cm from the cell axis and 2.) a centered high voltage feedthrough which transmitted the power, supplied through a power connector, to a hollow cathode inside the cell.

The axial hollow cathode glow discharge electrode assembly comprised a stainless steel plate (42 mm diameter, 0.9 mm thick) anode and a circumferential stainless steel cylindrical frame (5.08 cm OD, 7.2 cm long) perforated with evenly spaced 1 cm diameter holes. The cathode

was attached to the cell body by a stainless steel wire, and the cell body was grounded.

A 1.6 mm thick UV-grade sapphire window with 1.5 cm view diameter provided a visible light path from inside the cell. The viewing direction was normal to the cell axis.

Strontium (99.9 %) or magnesium (99.98 %) metal was coated onto the cathode in a glove box under a dry argon atmosphere. The cell was sealed in the glove box, removed, and then evacuated with a turbo vacuum pump to a pressure of 4 mtorr. The gas was ultrahigh purity hydrogen or noble gas-hydrogen mixture (90/10%) at 2 torr total pressure. The pressure of each test gas comprising a mixture with 10% hydrogen was determined by adding the pure noble gas to a given pressure and increasing the pressure with hydrogen gas to a final pressure. The partial pressure of the hydrogen gas was given by the incremental increase in total gas pressure monitored by a 0-10 torr absolute pressure gauge. The discharge was carried out under static gas conditions. The discharge was started and maintained by a DC electric field supplied by a constant voltage DC power supply at 275 V which produced a current of about 0.2 A. In the case of strontium-hydrogen and argon-hydrogen plasmas, the voltage was increased at 50 V increments from 275 V to 475 V, and the high resolution visible spectra were recorded to observe the effect of voltage on the Balmer α line broadening.

The plasma emission from the glow discharges of pure hydrogen and noble gas-hydrogen mixtures was fiber-optically coupled to the spectrometer through a 220F matching fiber adapter. The entrance and exit slits were set to 20 μm. The spectrometer was scanned between 656-657 nm using a 0.01 nm step size. The signal was recorded by a PMT with a stand alone high voltage power supply (950 V) and an acquisition controller. The data was obtained in a single accumulation with a 1 second integration time.

The electron density and temperature of the rt-plasma was determined using a compensated Langmuir probe according to the method given previously [24].

C. Power cell apparatus and procedure

Discharge plasma studies with 1.) hydrogen, argon, or argon-hydrogen mixture alone, 2.) hydrogen with strontium, sodium, magnesium, or barium, and 3.) argon-hydrogen mixture (77/23%) with strontium were carried out in the cylindrical stainless steel gas cell comprising a Type IV light source shown in Figure 4. The experimental setup for generating a glow discharge hydrogen plasma and for optically measuring the power balance is shown in Figure 5. The cell was heated in a 10 kW refractory brick kiln as shown in Figure 5. The cell was evacuated and pressurized with hydrogen, argon, or argon and hydrogen through a single 0.95 cm feed through. The discharge was started and maintained by an alternating current electric field in the 1.75 cm annular gap between an axial electrode and the cell wall. The cylindrical cell was 9.21 cm in diameter and 14.5 cm in height. The axial electrode was a 5.08 cm OD by 7.2 cm long stainless steel tube wound with several layers of nickel screen. The overall diameter of the axial electrode was 5.72 cm. Optical access to the cell was as described in section B except that an 8 mm quartz rod channeled the light from the view port through a stainless tube to a collimating lens which was focused on a 100 μm optical fiber located outside the furnace. Spectral data was recorded with a visible spectrometer and stored by a personal computer.

The field voltage was controlled by a variable voltage transformer operating from 115 VAC, 60 Hz. A step-up transformer was used when necessary. True rms voltage at the axial electrode was monitored by a digital multimeter. A second multimeter in series with the discharge gap was used to indicate the current. The cell temperature was measured by thermocouple probes located in the cell interior as described in section B. Pressure in the hydrogen and argon supply tube outside the furnace was monitored by 10 torr and 1000 torr absolute pressure gauges. In the absence of gas flow, the gas supply tube pressure was essentially the cell pressure. The pressure of each gas in an argon-hydrogen mixture was determined by adding one pure gas to a given pressure and increasing the pressure with a second gas to a final pressure. The partial pressure of the second gas was given by the incremental increase in total gas pressure.

Strontium (99.9 %), sodium (99.95 %), magnesium (99.98 %), or barium (99.99 %) metal was loaded into the cell under a dry argon atmosphere. The cell was evacuated with a turbo vacuum pump to a pressure of 4 mtorr during most of the heating process. During the heat-up the cell was periodically pressurized with hydrogen (99.999% purity) to approximately 100 torr and subsequently evacuated to purge gaseous contaminants from the system. When the cell temperature stabilized hydrogen was added until the steady pressure was approximately 1 torr. The field voltage was increased until breakdown occurred. This was confirmed by the spectrometer response to visible light emitted from the cell. The hydrogen or hydrogen-argon pressure was adjusted, as much as possible, to maximize the light emission from the cell. The voltage was maintained at the minimum level which resulted in a stable discharge during data acquisition.

The spectrometer system comprised a 100 μm optical fiber and visible spectrometer. To correct for the nonuniform response of the spectrometer system as a function of wavelength and the dependence of energy on wavelength, the system was calibrated against a reference light source. A spectral calibration factor was applied to the count rate data at each wavelength to yield the irradiation of the detector in units of energy/time/area/wavelength. The total visible radiant flux incident on the detector was calculated by integrating the spectral irradiation between 400 and 700 nm.

III. RESULTS

A. VUV spectroscopy

The cell was operated without any test material present to establish the baseline of the spectrometer. No emission was observed except for the low level blackbody filament radiation at the longer wavelengths. The intensity of the Lyman α emission as a function of time and the VUV/UV/VIS spectra ($40-560\,nm$) was observed at 700°C from the gas cell comprising a tungsten filament, a titanium dissociator, and 1.) hydrogen, argon, neon, or helium alone, 2.) sodium, magnesium, or barium metal, 3.) sodium, magnesium, or barium metal with 300 mtorr

hydrogen with a flow rate of 5.5 sccm. No emission was observed in any case. The maximum filament power was greater than 500 watts. A metal coating formed in the cap of the cell over the course of the experiment in each case with a metal vaporized by filament heating.

The intensity of the Lyman α emission as a function of time from the gas cell at a cell temperature of 700°C comprising a tungsten filament, a titanium dissociator, vaporized strontium metal, and 300 mtorr hydrogen at a flow rate of 5.5 sccm is shown in Figure 6. Strong emission was observed from vaporized strontium and hydrogen. The VUV spectrum ($90-130\,nm$) of the cell emission recorded at about the point of the maximum Lyman α emission is shown in Figure 7. No emission was observed in the absence of hydrogen flow. A metal coating formed in the cap of the cell over the course of the experiment.

Hydrogen was replaced by a 97% argon and 3% hydrogen mixture at a total flow rate of 5.5 sccm. The intensity of the Lyman α emission as a function of time and the VUV spectra ($40-160\,nm$) at 700°C was observed for the gas cell comprising a tungsten filament and 1.) 300 mtorr argon-hydrogen mixture (97/3%) and 2.) vaporized sodium, magnesium, or barium metal with 300 mtorr argon-hydrogen mixture (97/3%). No emission was observed in any case.

The VUV spectrum ($80-130\,nm$) of the cell emission recorded at about the point of the maximum Lyman α emission from the gas cell at a cell temperature of 700°C comprising a tungsten filament, vaporized strontium metal, and 300 mtorr argon-hydrogen mixture (97/3%) is shown in Figure 8. Strong VUV emission was observed that was more intense than with hydrogen and strontium. The Lyman series corresponding to atomic hydrogen emission and strong Ar II ion emission was observed at 92.0 nm and 93.2 nm.

The rt-plasma required the presence of hydrogen. The zero order emission in the VUV was observed with titration of increasing partial pressure of hydrogen added to argon gas. It was found that increasing the hydrogen pressure initially increased the atomic hydrogen emission lines, but with increasing hydrogen partial pressure at a constant total pressure, the Ar II emission in the VUV at 92.0 nm and 93.2 nm decreased which resulted in a decrease of the plasma intensity including the hydrogen emission. The optimum argon-hydrogen gas mixture which

produced the greatest emission was determined to be 95% argon and 5% hydrogen which is similar to the 97% argon and 3% hydrogen mixture of Grimm-type discharges studied by Kuraica and Konjevic [8] and Videnovic et al. [9]. The optimum ratio was consistent with a rt-discharge mechanism which required maximum concentrations of both atomic hydrogen and Ar^+.

B. VUV Emission of Sr^+ Catalyst and Ar^+ Catalyst Formed with Strontium

The second and third ionization energies of strontium are $11.03013\,eV$ and $42.89\,eV$, respectively [22]. The ionization reaction of Sr^+ to Sr^{3+}, then, has a net enthalpy of reaction of $53.92\,eV$, which is about $2 \cdot 27.2\,eV$; thus, Sr^+ may serve as a catalyst to form an rt-plasma. The VUV spectrum ($35-67\,nm$) of the emission of a strontium rt-plasma Type I light source is shown in Figure 9. Line emission corresponding to Sr^{3+} that confirmed the catalyst mechanism was observed at $66.4\,nm$, $41.35\,nm$, and $39.6\,nm$. which matched NIST tables [25]. Sr^{2+} was observed at $56.3\,nm$, $51.4\,nm$, $49.2\,nm$, and $43.7\,nm$. The presence of the Sr^+ catalyst was confirmed by the Sr^+ line emission shown in Figure 10 at $407.77\,nm$ which matched NIST tables [25].

The VUV spectra ($30-170\,nm$) and ($20-62.5\,nm$) of the emission of a strontium-argon-hydrogen rt-plasma Type I light source and a control hydrogen microwave plasma Type II light source are shown in Figures 11 and 12, respectively. The standard VUV emission spectrum ($38-50\,nm$) of an argon microwave plasma recorded on the McPherson 4° grazing incidence VUV spectrometer (Model 248/310G) with a CEM is shown in Figure 13. A broad continuum radiation band in the region of $45.6\,nm$ was observed in the strontium-argon-hydrogen gas cell emission that was not present in the control hydrogen or argon plasmas. This emission was dramatically different from that given by a microwave plasma of argon wherein the entire Rydberg series of lines of Ar^+ was observed with a discontinuity of the series at the limit of the ionization energy of Ar^+ to Ar^{2+} at $44.9\,nm$. In addition, an intense Rydberg series of lines in the region 110-130 nm was observed in the strontium-argon-hydrogen gas cell emission as shown in Figure 11. The lines were not present in the

control hydrogen or argon plasmas, and were only observed with strontium present with argon and hydrogen. The series was assigned to Ar^+ transitions which are reported in the Journal of Physical and Chemical Reference Data [26].

C. Line broadening measurements Type I cells

The results of the 656.3 nm Balmer α line width measured with a high resolution ($\pm 0.006\,nm$) visible spectrometer on light emitted from rt-plasmas of hydrogen with $SrCO_3$ and $SrCO_3$ with an argon-hydrogen mixture (97/3%) maintained in Type I cells are shown in Figures 14 and 15, respectively. The Balmer α line width and energetic hydrogen atom densities and energies given in Table I were calculated using the method of Videnovic et al. [9]. Significant line broadening of 14 and 24 eV and atom densities of $8\,X\,10^{11}$ *and* $4\,X\,10^{11}\,atoms/cm^3$ were observed from a rt-plasma of hydrogen formed with strontium, and strontium with Ar^+ catalysts, respectively. A glow discharge of hydrogen maintained at the same total pressure showed no excessive broadening corresponding to an average hydrogen atom temperature of $\approx 3\,eV$. The superposition of the 656.3 nm Balmer α line width recorded with a high resolution ($\pm 0.006\,nm$) visible spectrometer on a hydrogen-strontium rt-plasma and a hydrogen-strontium rt-plasma intensified by argon ion catalyst is shown in Figure 16. By comparison to the strontium rt-plasma, significant broadening attributable to argon ion was observed corresponding to an average hydrogen atom temperature of $24\,eV$ versus $14\,eV$. The atom density was also very high in the argon rt-plasma given that the hydrogen concentration was 30 times less than that of the strontium-pure-hydrogen rt-plasma.

D. Line broadening measurements on Type III cells

The 656.3 nm Balmer α line width was measured on Type III light sources normal to the applied electric field direction with a high resolution ($\pm 0.025\,nm$) visible spectrometer. The discharge was started and maintained at 2 Torr total pressure by a DC electric field supplied by a constant voltage DC power supply at 275 V which produced a current of

about 0.2 A. The results of the gas discharge plasmas of a mixture of 10% hydrogen and 90% xenon, strontium with hydrogen and 10% hydrogen with helium or argon and strontium each compared to control hydrogen alone are given in Figures 17-20, respectively. In addition, the emission of a strontium-argon plasma in the region of the Balmer α line was recorded as shown in Figure 20. Sr I emission was observed at 655 nm, but, no emission was observed in the region of the Balmer α line which eliminated the possibility that a strontium line close to the Balmer α line was the source of the line broadening with strontium present. The Balmer α line width and energetic hydrogen atom densities and energies are given in Table I. It was found that strontium-hydrogen, helium-hydrogen, argon-hydrogen, strontium-helium-hydrogen, and strontium-argon-hydrogen plasmas showed significant broadening corresponding to an average hydrogen atom temperature of $23\text{-}45\,eV$; whereas, pure hydrogen, krypton-hydrogen, xenon-hydrogen, and magnesium-hydrogen showed no excessive broadening corresponding to an average hydrogen atom temperature of $\approx 4\,eV$. No voltage effect was observed with the argon-hydrogen and strontium-hydrogen plasmas.

E. Optically measured power balance

The count rate and spectrometer system irradiation of the background spectrum of hydrogen and strontium vapor over the wavelength range $400 \le \lambda \le 700\,nm$ in the absence of power applied to the electrode and in the absence of a discharge was measured. This data was collected during cell evacuation following the test with strontium and hydrogen at a cell temperature of 664°C. The maximum visible irradiation of $0.004\,\mu W/cm^2 nm$ occurred at the red end of the visible spectrum. The results are summarized in Table II where T is the temperature, P_{hyd} and P_{Ar} are the hydrogen and argon partial pressures, and P_v is the equilibrium metal vapor pressure calculated from standard curves of the vapor pressure as a function of temperature [27].

Power was applied to the electrode to achieve a bright plasma in the strontium-hydrogen mixture and the controls of hydrogen alone, and sodium-hydrogen, magnesium-hydrogen, and barium-hydrogen mixtures for cell temperatures in the range 335-666°C. In each case, the spectral

radiant flux at the spectrometer system was recorded. If possible, the power driving the controls was adjusted such that the peak spectrometer system spectral irradiation was about $0.1\ \mu W/cm^2nm$ in each case. The integrated visible irradiation levels were of the order of $1\ \mu W/cm^2$. One exception was the case of hydrogen-barium. In this case, the maximum spectral irradiation levels and integrated visible irradiation levels were only of the order of $0.01\ \mu W/cm^2nm$ and $0.03\ \mu W/cm^2$, respectively.

The power required to maintain a plasma of equivalent optical brightness with strontium atoms present was 4000, 7000, and 6500 times less than that required for the sodium, magnesium, and barium control, respectively. A driving power of 33.7 W and 58 W was necessary to achieve a total visible radiant flux of about $1\ \mu W/cm^2$ from a sodium-hydrogen mixture and a magnesium-hydrogen mixture, respectively. For a hydrogen-barium mixture, a power input of about 55 W was required to achieve a total visible irradiation of about $0.03\ \mu W/cm^2$. Whereas, in the case of a strontium-hydrogen mixture, a power input of 8.5 mW resulted in a plasma with a total visible radiant flux of about the same optical brightness as sodium and magnesium. A plasma formed at a cell voltage of about 250 V for hydrogen alone and sodium-hydrogen mixtures, and 140-150 V for hydrogen-magnesium and hydrogen-barium mixtures; whereas, a plasma formed for hydrogen-strontium mixtures at the extremely low voltage of about 2 V. The results are summarized in Table II.

Power was applied to the electrode to achieve a bright plasma in the strontium-argon-hydrogen mixture and the controls of argon alone and argon-hydrogen alone for cell temperatures in the range 514-520°C. In each case, the spectral radiant flux at the spectrometer system was recorded. If possible, the power driving the controls was adjusted such that the peak spectrometer system spectral irradiation was about $0.1\ \mu W/cm^2nm$ in each case. The integrated visible irradiation levels were of the order of $1\ \mu W/cm^2$.

The power required to maintain a plasma of equivalent optical brightness with strontium atoms present was 8600 and 6300 times less than that required for argon-hydrogen and argon control, respectively. A driving power of 33.5 W and 24.7 W was necessary to achieve a total visible radiant flux of about $1\ \mu W/cm^2$ from an argon-hydrogen mixture

and argon, respectively. Whereas, in the case of a strontium-argon-hydrogen mixture, a power input of 4 mW resulted in a plasma with a total visible radiant flux of about the same optical brightness as the argon-hydrogen mixture and argon. A plasma formed at a cell voltage of 224 V for an argon-hydrogen mixture alone, and 190 V for argon alone; whereas, a plasma formed for argon-hydrogen-strontium mixtures at an extremely low voltage of about 6.6 V. The results are summarized in Table II.

The count rate and the spectrometer system irradiation for a mixture of hydrogen and strontium vapor at 664°C is shown in Figure 21. Optimal light emission was observed after several hours of cell evacuation. The hydrogen partial pressure was unknown under these conditions. The calculated equilibrium vapor pressure of strontium at 664°C is approximately 270 mtorr. The measured breakdown voltage was approximately 2 V. The maintenance voltage for a stable discharge was 2.2 V and input power was 8.5 mW. Spectral characteristics are noted in Table III. The hydrogen Balmer α and β peaks were obscured by strong strontium emission near 654.7 and 487.2 nm, respectively.

The spectrometer system irradiation for a hydrogen discharge at a cell temperature of 664°C and 1 torr is shown in Figure 22. The breakdown voltage was approximately 220 V. The field voltage required to form a stable discharge was 224 V. The input power was 24.6 W. Spectral features are tabulated in Table IV. The peak at 589.1 nm may be due to sodium contamination from a previous experimental run. The minor peaks at 518.2 and 558.7 nm have not been identified.

The spectrometer system irradiation for mixtures of hydrogen and sodium vapor are shown in Figures 23a-c for temperatures of 335, 516, and 664°C, respectively. Corresponding hydrogen pressures are 1, 1.5, and 1.5 torr, respectively. The calculated sodium vapor pressure was 51 mtorr, 5.3 torr, and 63 torr at 335, 516, and 664°C, respectively. At least 200 V was required to maintain a discharge. The input power for a stable discharge ranged from approximately 10 W at 664°C to 34 W at 335°C. Spectral features corresponding to 335°C are summarized in Table V. Strong emission observed near 656-657 nm was probably due, in-part, to hydrogen. The relative contribution to the intensity was masked by strong sodium emission at a slightly shorter wavelength. The peak at

486.2 nm could only be due to hydrogen emission. Sodium does not have emission lines in the neighborhood of this wavelength. The intensity of this peak diminishes relative to the more prominent sodium peaks with increasing temperature as shown in Figures 23a-c. This may have been due to a decreasing hydrogen concentration as the sodium vapor pressure increased.

The spectral response for mixtures of magnesium vapor and hydrogen are shown in Figures 24a-c for temperatures of 449, 582, and 654°C, respectively. The corresponding hydrogen pressures are 4, 4.2, and 3 torr, respectively. A minimum of 150 V was required to maintain a discharge. The minimum input power required to maintain a stable discharge was 58 W at 449°C. Spectral features corresponding to 449°C are summarized in Table VI. Both hydrogen and magnesium spectral features are observed. The modest sodium emission at 588 nm may be due to sodium contamination from previous control experiments.

The spectral response for a mixture of barium vapor and hydrogen at 666°C is shown in Figure 25. The hydrogen partial pressure and barium vapor pressure are 2 torr and 25 mtorr, respectively. It was not possible to achieve a total visible irradiation level of $1\ \mu W/cm^2$ even with voltages approaching 150 V. The voltage and power input corresponding to Figure 25 are 138 V and 55 W, respectively. Spectral features are summarized in Table VII. Both barium and hydrogen spectral features are observed as well as sodium features which are presumably due to contamination. The peak at 493 nm has not been identified.

The spectral response for a mixture of hydrogen, argon, and strontium vapor at 514°C is shown in Figure 26. The hydrogen and argon partial pressures were 0.3 and 1 Torr, respectively. The strontium vapor pressure was approximately 6 mtorr at this temperature. The voltage required for a stable discharge was 6.6 V. The corresponding power input to the cell was approximately 4 mW. The spectral characteristics are tabulated in Table VIII. The two major features were due to strontium emission. The very minor spectral features at 639 and 654 nm were due to argon. The total visible irradiation of the spectrometer detector was 1.3 $\mu W/cm^2$. The spectral responses for a mixture of argon and hydrogen and for pure argon are shown in Figures 27 and 28, respectively. For irradiation levels in the range 1-2 $\mu W/cm^2$, voltages of

224 and 190 V and power inputs of 33.5 and 24.7 W were required for discharges in argon and hydrogen, and pure argon, respectively. The spectral characteristics are tabulated in Tables IX and X for these gas discharges. In the case of pure argon, the emission at 656 nm was most likely hydrogen Balmer alpha emission due to some hydrogen contamination.

IV. DISCUSSION

Intense VUV emission was observed at low temperatures (e.g. $\approx 10^3\ K$) from atomic hydrogen and strontium which ionizes at an integer multiple of the potential energy of atomic hydrogen. The emission intensity of the rt-plasma generated by strontium increased significantly with the introduction of argon gas only when Ar^+ emission was observed. The ionization energy of Ar^+ to Ar^{2+} is $27.6\ eV$. In the cases where Lyman α emission was observed, no possible chemical reactions of the tungsten filament, the dissociator, the vaporized strontium, and 300 mtorr hydrogen or argon-hydrogen mixture at a cell temperature of 700°C could be found which accounted for the hydrogen α line emission. In fact, no known chemical reaction releases enough energy to excite Lyman α emission from hydrogen. The emission was not observed with hydrogen or an argon-hydrogen mixture alone or with helium, neon, or argon gas. Intense emission was observed for strontium with hydrogen gas, but no emission was observed with hydrogen or strontium alone. This result indicates that the emission may be due to a reaction of hydrogen. The increase in intensity with the formation of Ar^+ and the equal dependency of the emission on the presence of both Ar^+ and atomic hydrogen indicates a reaction between these species. A similar effect reported previously [15] was also observed when helium was added to a hydrogen plasma which depended on the presence of He^+ and atomic hydrogen.

The characteristic emission from Sr^+ and Sr^{3+} confirmed the resonant nonradiative energy transfer of $2 \cdot 27.2\ eV$ from atomic hydrogen to Sr^+. Atomic strontium may serve as a catalyst as well which may initiate the rt-plasma and form Sr^+ [15]. With a highly conductive plasma, the voltage of the cell was about 20 V, and the field strength was

about 1-2 V/cm which was too low to ionize Sr^+ to Sr^{3+} which requires at least $53.92\,eV$, rather a resonant energy transfer explains the observations.

Characteristic emission was also observed from a continuum state of Ar^{2+} which confirmed the resonant nonradiative energy transfer of $27.2\,eV$ from atomic hydrogen Ar^+. In the rt-plasma due to the presence of Ar^+, atomic hydrogen may resonantly transfer energy to Ar^+ to cause its ionization to Ar^{2+} which may then decay and emit the radiation. The vacuum reaction in the absence of an electric field is

$$Ar^{2+} + e^- \rightarrow Ar^+ + 27.63\,eV \qquad (3)$$

In the catalysis of atomic hydrogen by Ar^+, a weak electric field may adjust the energy of ionizing Ar^+ to Ar^{2+} to match the energy of $27.2\,eV$ to permit the catalysis. The transfer of $27.2\,eV$ from atomic hydrogen to Ar^+ in the presence of the weak field of the filament results in its excitation to a continuum state. Then, the energy for the transition from essentially the Ar^{2+} state to the lowest state of Ar^+ is predicted to give a broad continuum radiation in the region of $45.6\,nm$. This broad continuum emission was observed. This emission was dramatically different from that given by an argon microwave plasma wherein the entire Rydberg series of lines of Ar^+ was observed with a discontinuity of the series at the limit of the ionization energy of Ar^+ to Ar^{2+}. The observed Ar^+ continuum in the region of $45.6\,nm$ confirms the catalyst mechanism of the rt-plasma.

Line broadening of the hydrogen Balmer lines provides a sensitive measure of the number and energy of excited hydrogen atoms in a plasma. To further characterize the plasma parameters of rt-plasmas, the width of the 656.3 nm Balmer α line was recorded on light emitted from rt-plasmas formed from hydrogen with a gaseous ion which ionizes at integer multiples of the potential energy of atomic hydrogen. The energetic hydrogen atom densities and energies were determined from the broadening, and it was found that significant line broadening of 14 and 24 eV and an atom density of $8 X 10^{11}$ *and* $4 X 10^{11}\ atoms/cm^3$ were observed from a rt-plasma of hydrogen formed with strontium, and strontium with Ar^+ catalysts, respectively. Whereas, a glow discharge of hydrogen maintained at the same total pressure with an electric field strength that was at least two order of magnitude greater than the l

V/cm field of the filament cell showed no excessive broadening corresponding to an average hydrogen atom temperature of $\approx 3\,eV$.

In the characterization of argon-hydrogen (97/3%) Grimm-type plasma discharges with a hollow anode, M. Kuraica and N. Konjevic [8] and Videnovic et al. [9] analyzed the broadening data in terms of Stark and Doppler effects wherein acceleration of charges such as H^+, H_2^+, and H_3^+ in the high fields (e. g. over $10\,kV/cm$) which were present in the cathode fall region was used to explain the Doppler component. In our experiments with Type I cells, the measured field of the incandescent heater was extremely weak, 1 V/cm, corresponding to a broadening much less than $1\,eV$. Thus, we have assumed that Doppler broadening due to thermal motion was the dominant source in the rt-plasmas to the extent that other sources may be neglected. In general, the experimental profile is a convolution of two Doppler profiles, an instrumental profile, the natural (lifetime) profile, Stark profiles, van der Waal's profiles, a resonance profile, and fine structure. The source of broadening was confirmed to be Doppler alone by considering each possible source according to the methods described previously [31-32]. For example, using a compensated Langmuir probe [24], the electron density was measured to be $n_e < 10^{10}\,cm^{-3}$ which is at least five orders of magnitude too low to invoke Stark broadening as discussed previously [31-32].

It was reported previously [31-32] that microwave helium-hydrogen and argon-hydrogen plasmas showed extraordinary broadening corresponding to an average hydrogen atom temperature of 180-210 eV and 110-130 eV, respectively. Whereas, pure hydrogen and xenon-hydrogen microwave plasmas showed no excessive broadening corresponding to an average hydrogen atom temperature of $\approx 4\,eV$. No hydrogen species, H^+, H_2^+, H_3^+, H^-, H, or H_2, responds to the microwave field; rather, only the electrons respond. But, the measured electron temperature was about 1 eV which requires that $T_H >>> T_e$. This result can not be explained by electron or external Stark broadening or electric field acceleration of charged species. The electron density was five orders of magnitude too low [31-32] for detectable Stark broadening. And, in microwave driven plasmas, there is no high electric field in a cathode fall region ($> 1kV/cm$) to accelerate positive ions as proposed previously [9, 33-35] to explain significant broadening in hydrogen containing plasmas

driven at a high voltage electrodes. It is impossible for H or any H-containing ion which may give rise to H to have a higher temperature than the electrons in a microwave plasma. The observation of excessive Balmer line broadening in a microwave driven plasma requires a source of energy other than that provided by the electric field. The formation of fast H was explained by a resonance energy transfer between hydrogen atoms and Ar^+ or He^+ of an integer multiple of the potential energy of atomic hydrogen, $27.2\,eV$. Similarly, the source of the excessive line broadening in the strontium and argon-strontium rt-plasma is consistent with that of VUV emission, an energetic reaction caused by a resonance energy transfer between hydrogen atoms and strontium or Ar^+ catalysts.

An rt-plasma with hydrogen-potassium mixtures has been reported in an experiment identical to the present VUV experiments [18] with Type I cells. In this experiment and the one treated in reference [17], a rt-plasma formed with hydrogen-potassium mixtures wherein the plasma decayed with a two second half-life when the electric field was set to zero [17]. This was the thermal decay time of the filament which dissociated molecular hydrogen to atomic hydrogen. This experiment showed that hydrogen line emission was occurring even though the voltage between the heater wires was set to and measured to be zero and indicated that the emission was due to a reaction of potassium atoms with atomic hydrogen. Potassium atoms ionize at an integer multiple of the potential energy of atomic hydrogen, $m \cdot 27.2\,eV$. The enthalpy of ionization of K to K^{3+} has a net enthalpy of reaction of $81.7426\,eV$, which is equivalent to $m = 3$. The observation of K^{3+} has been reported previously [13].

A rt-plasma of hydrogen and certain alkali ions formed at low temperatures ($<10^3\,K$) as recorded via VUV spectroscopy and the hydrogen Balmer and alkali line emissions in the visible range [18]. The observed plasma formed from atomic hydrogen generated at a tungsten filament that heated a titanium dissociator and one of potassium, rubidium, cesium, and their carbonates and nitrates. These atoms and ions ionize to provide a net enthalpy of reaction of an integer multiple of the potential energy of atomic hydrogen ($m \cdot 27.2\,eV$, $m = integer$) to within 0.17 eV and comprise only a single ionization in the case of a potassium or rubidium ion. Whereas, the chemically similar atoms of sodium and

sodium and lithium carbonates and nitrates which do not ionize with these constraints caused no emission. To test the electric dependence of the emission, the weak electric field of about 1 V/cm was set and measured to be zero in $< 0.5 X 10^{-6}$ sec. An afterglow duration of about one to two seconds was recorded in the case of potassium, rubidium, cesium, K_2CO_3, $RbNO_3$, and $CsNO_3$. Hydrogen line or alkali line emission was occurring even though the voltage between the heater wires was set to and measured to be zero. These atoms and ions ionize to provide a net enthalpy of reaction of an integer multiple of the potential energy of atomic hydrogen to within less than the thermal energies at $\approx 10^3 K$ and comprise only a single ionization in the case of a potassium or rubidium ion. Since the thermal decay time of the filament for dissociation of molecular hydrogen to atomic hydrogen was similar to the rt-plasma afterglow duration, the emission was determined to be due to a reaction of atomic hydrogen with each of the atoms or ions that did not require the presence of an electric field to be functional.

The width of the 656.3 nm Balmer α line emitted from gas discharge plasmas having atomized hydrogen from pure hydrogen alone, hydrogen with magnesium or strontium, a mixture of 10% hydrogen and helium, argon, krypton, or xenon, and a mixture of 10% hydrogen and helium or argon with strontium was also measured with a high resolution ($\pm 0.025 nm$) visible spectrometer on light emitted from Type III cells. The energetic hydrogen atom density and energies were determined from the broadening, and it was found that strontium-hydrogen, helium-hydrogen, argon-hydrogen, strontium-helium-hydrogen, and strontium-argon-hydrogen plasmas showed significant broadening corresponding to an average hydrogen atom temperature of 23-45 eV; whereas, pure hydrogen, krypton-hydrogen, xenon-hydrogen, and magnesium-hydrogen showed no excessive broadening corresponding to an average hydrogen atom temperature of $\approx 4 eV$. Thus, line broadening was only observed for the atoms and ions which provided a net enthalpy of reaction of a multiple of the potential energy of the hydrogen atom.

In our normal glow discharge studies with argon-hydrogen plasmas, the voltage was increased at 50 V increments from 275 V to 475 V, and the high resolution visible spectra were recorded to observe the effect of voltage on the Balmer α line broadening. In contrast to an

increase in broadening with voltage predicted by Kuraica and Konjevic [8], no voltage effect was observed. Also, no voltage effect was also observed with the strontium-hydrogen plasma which supports the rt-plasma mechanism of the low voltage strontium-hydrogen and strontium-argon-hydrogen plasmas reported in the Optically measured power balance section.

Since line broadening is a measure of the atom temperature, and a significant increase was observed for strontium or argon with hydrogen, the power balance of a gas cell having vaporized strontium and atomized hydrogen from pure hydrogen or argon-hydrogen mixture (77/23%) was measured by integrating the total light output corrected for spectrometer system response and energy over the visible range. A cylindrical nickel mesh hydrogen dissociator of a gas cell also served as an electrode to produce an essentially uniform radial electric field between the dissociator and the wall of the cylindrical stainless steel gas cell. Power was applied to the electrode to achieve a bright plasma which was recorded over the wavelength range $400 \leq \lambda \leq 700\ nm$. Control experiments were identical except that sodium, magnesium, or barium replaced strontium. In the case of hydrogen-sodium, hydrogen-magnesium, and hydrogen-barium mixtures, 4000, 7000, and 6500 times the power of the hydrogen-strontium mixture was required, respectively, in order to achieve that same optically measured light output power. With the addition of argon to the hydrogen-strontium plasma, the power required to achieve that same optically measured light output power was reduced by a factor of about two. In the case of an argon-hydrogen mixture and argon alone, the power requirement was 8600 and 6300 times the power input of the argon-hydrogen-strontium mixture, respectively. A plasma formed at a cell voltage of about 250 V for hydrogen alone and sodium-hydrogen mixtures, 140-150 V for hydrogen-magnesium and hydrogen-barium mixtures, 224 V for an argon-hydrogen mixture alone, and 190 V for argon alone; whereas, a plasma formed for hydrogen-strontium mixtures and argon-hydrogen-strontium mixtures at extremely low voltages of about 2 V and 6.6 V, respectively. This is two orders of magnitude lower than the starting voltages measured for gas glow discharges, cf. Table XI.

The observation of rt-plasmas formed with strontium and argon at

1% of the theoretical or prior known voltage requirement with a light output per unit power input up to 8600 times that of the control standard light source has implications for an advanced light source.

ACKNOWLEDGMENT

Special thanks to Jobin Yvon Horiba, Inc, Edison, NJ for use of the high resolution visible spectrometer, to Takeyoshi Onuma and Ying Lu for recording VUV spectra, and to Bala Dhandapani and Jiliang He for reviewing this manuscript.

REFERENCES

1. J. A. R. Sampson, *Techniques of Vacuum Ultraviolet Spectroscopy*, Pied Publications, (1980), pp. 94-179.
2. P. W. J. M. Boumans, Spectrochim. Acta Part B, 46 (1991) 711.
3. J. A. C. Broekaert, Appl. Spectrosc., 49, (1995) 12A.
4. P. W. J. M. Boumans, J. A. C. Broekaert, and R. K. Marcus, Eds., Spectrochim. Acta Part B, 46 (1991) 457.
5. M. Dogan, K. Laqua, and H. Massmann, "Spektrochemische Analysen mit einer Glimmentladungslampe als Lichtquelle—I," Spectrochim. Acta, Volume 26B, (1971) 631–649.
6. M. Dogan, K. Laqua, and H. Massmann, "Spektrochemische Analysen mit einer Glimmentladungslampe als Lichtquelle—II, "Spectrochim. Acta, Volume 27B, (1972) 65–88.
7. J. A. C. Broekaert, J. Anal. At. Spectrom., 2 (1987) 537.
8. M. Kuraica, N. Konjevic, "Line shapes of atomic hydrogen in a plane-cathode abnormal glow discharge", Physical Review A, Volume 46, No. 7, October (1992), pp. 4429-4432.
9. I. R. Videnovic, N. Konjevic, M. M. Kuraica, "Spectroscopic investigations of a cathode fall region of the Grimm-type glow discharge", Spectrochimica Acta, Part B, Vol. 51, (1996), pp. 1707-1731.
10. P. Kurunczi, H. Shah, and K. Becker, "Hydrogen Lyman-α and Lyman-β emissions from high-pressure microhollow cathode discharges in $Ne-H_2$ mixtures", J. Phys. B: At. Mol. Opt. Phys., Vol. 32, (1999), L651-L658.
11. M. Parker and R. K. Marcus, Appl. Spectrosc., 48, (1994) 623.
12. J. A. R. Sampson, *Techniques of Vacuum Ultraviolet Spectroscopy*, Pied Publications, (1980), pp. 94-179.
13. R. Mills, P. Ray, "Spectroscopic Identification of a Novel Catalytic Reaction of Potassium and Atomic Hydrogen and the Hydride Ion Product", Int. J. Hydrogen Energy, Vol. 27, No. 2, February, (2002), pp. 183-192.
14. R. Mills, "Spectroscopic Identification of a Novel Catalytic Reaction of Atomic Hydrogen and the Hydride Ion Product", Int. J. Hydrogen Energy, Vol. 26, No. 10, (2001), pp. 1041-1058.
15. R. Mills and M. Nansteel, "Argon-Hydrogen-Strontium Discharge Light

Source", IEEE Transactions on Plasma Science, in press.
16. R. Mills, J. Dong, Y. Lu, "Observation of Extreme Ultraviolet Hydrogen Emission from Incandescently Heated Hydrogen Gas with Certain Catalysts", Int. J. Hydrogen Energy, Vol. 25, (2000), pp. 919-943.
17. R. Mills, "Temporal Behavior of Light-Emission in the Visible Spectral Range from a Ti-K2CO3-H-Cell", Int. J. Hydrogen Energy, Vol. 26, No. 4, (2001), pp. 327-332.
18. R. Mills, T. Onuma, and Y. Lu, "Formation of a Hydrogen Plasma from an Incandescently Heated Hydrogen-Catalyst Gas Mixture with an Anomalous Afterglow Duration", Int. J. Hydrogen Energy, Vol. 26, No. 7, July, (2001), pp. 749-762.
19. R. Mills, M. Nansteel, and Y. Lu, "Observation of Extreme Ultraviolet Hydrogen Emission from Incandescently Heated Hydrogen Gas with Strontium that Produced an Anomalous Optically Measured Power Balance", Int. J. Hydrogen Energy, Vol. 26, No. 4, (2001), pp. 309-326.
20. R. L. Mills, P. Ray, B. Dhandapani, M. Nansteel, X. Chen, J. He, "New Power Source from Fractional Rydberg States of Atomic Hydrogen", Chem. Phys. Letts., in press.
21. R. Mills, P. Ray, "Spectral Emission of Fractional Quantum Energy Levels of Atomic Hydrogen from a Helium-Hydrogen Plasma and the Implications for Dark Matter", Int. J. Hydrogen Energy, Vol. 27, No. 3, pp. 301-322.
22. David R. Linde, *CRC Handbook of Chemistry and Physics*, 79 th Edition, CRC Press, Boca Raton, Florida, (1998-9), p. 10-175 to p. 10-177.
23. R. L. Mills, A. Voigt, P. Ray, M. Nansteel, B. Dhandapani, "Measurement of Hydrogen Balmer Line Broadening and Thermal Power Balances of Noble Gas-Hydrogen Discharge Plasmas", Int. J. Hydrogen Energy, Vol. 27, No. 6, (2002), pp. 671-685.
24. D. Barton, J. W. Bradley, D. A. Steele, and R. D. Short, "Investigating radio frequency plasmas used for the modification of polymer surfaces," J. Phys. Chem. B, Vol. 103, (1999), pp. 4423-4430.
25. NIST Atomic Spectra Database, www.physics.nist.gov/cgi-bin/AtData/display.ksh.
26. R. Kelly, Journal of Physical and Chemical Reference Data. "Atomic and Ionic Spectrum Lines below 2000 Angstroms: Hydrogen through Krypton", Part I (H-Cr), Volume 16, (1987), Supplement No. 1,

Published by the American Chemical Society and the American Institute of Physics for the National Bureau of Standards, pp. 392-396.
27. C. L. Yaws, *Chemical Properties Handbook*, McGraw-Hill, (1999).
28. D. R. Linde, *CRC Handbook of Chemistry and Physics*, 79 th Edition, CRC Press, Boca Raton, Florida, (1998-9), pp. 10-1 to p. 10-87.
29. A. von Engel, *Ionized Gases*, American Institute of Physics, (1965).
30. M. S. Naidu and V. Kamaraju, *High Voltage Engineering*, McGraw-Hill, (1996).
31. R. L. Mills, P. Ray, "Substantial Changes in the Characteristics of a Microwave Plasma Due to Combining Argon and Hydrogen", New Journal of Physics, www.njp.org, Vol. 4, (2002), pp. 22.1-22.17.
32. R. L. Mills, P. Ray, B. Dhandapani, J. He, "Comparison of Excessive Balmer α Line Broadening of Glow Discharge and Microwave Hydrogen Plasmas with Certain Catalysts", J. of Applied Physics, submitted.
33. S. Alexiou, E. Leboucher-Dalimier, "Hydrogen Balmer-α in dense plasmas", Phys, Rev. E, Vol. 60, No. 3, (1999), pp. 3436-3438.
34. S. Djurovic, J. R. Roberts, "Hydrogen Balmer alpha line shapes for hydrogen -argon mixtures in a low-pressure rf discharge", J. Appl. Phys., Vol. 74, No. 11, (1993), pp. 6558-6565.
35. S. B. Radovanov, K. Dzierzega, J. R. Roberts, J. K. Olthoff, Time-resolved Balmer-alpha emission from fast hydrogen atoms in low pressure, radio-frequency discharges in hydrogen", Appl. Phys. Lett., Vol. 66, No. 20, (1995), pp. 2637-2639.

Table I. Energetic hydrogen atom densities and energies for rt-plasmas and ordinary hydrogen plasmas maintained in Type I and Type III light sources.

Plasma Gas	Light Source Type	Hydrogen Atom Density[a] (10^{12} *atoms*/cm^3)	Hydrogen Atom Energy[b] (eV)
H_2	III	50	3-5
Mg/H_2	III	60	4-5
Kr/H_2	III	10	2.5-3.5
Xe/H_2	III	10	3-4
Sr/H_2	III	100	23-25
Ar/H_2	III	30	30-35
He/H_2	III	30	33-38
$Sr/Ar/H_2$	III	40	35-40
$Sr/He/H_2$	III	40	40-45
Sr/H_2	I	0.8	14
$Sr/Ar/H_2$	I	0.4	24

[a] Approximate calculated after [9], Eqs. (1-2).

[b] Calculated after [9], Eqs. (1-2).

Table II. Type IV light source discharge conditions and comparison of the driving power to achieve a total visible radiant flux of about 1 $\mu W/cm^2$.

	T (°C)	P_{hyd} (torr)	P_{Ar} (torr)	P_v (torr)[a]	Voltage (V)	Current (mA)	Integ. time (ms)	Detector irradiation ($\mu W/cm^2$)	Power (W)
Ar+H_2+Sr	514	0.3	1.0	0.006	6.56	0.6	204	1.3	0.0039
Ar+H_2	519	0.295	0.5	- - - -	224	184	409	1.9	33.5[b]
Ar	520	- - - -	1.0	- - - -	190	170	307	1.1	24.7[b]
H_2+Sr	664	- - - -		0.270	2.20	3.86	768	1.17	0.0085
H_2	664	1.0		- - - -	224	110	1130	2.08	24.6
H_2+Na	335	1.0		0.051	272	124	122	1.85	33.7
H_2+Na	516	1.5		5.3	220	68	768	0.40	15.0
H_2+Na	664	1.5		63	240	41	768	0.41	9.84
H_2+Mg	449	4.0		0.016	153	380	500	1.7	58
H_2+Mg	582	4.2		0.6	233	290	500	0.16	68
H_2+Mg	654	3.0		2.8	250	400	1000	0.18	100.0
H_2+Ba	666	2.0		0.025	138	730	716	0.03	55[b]
Bkgnd.	664	- - - -		0.270	0	0	768	0.20	0

[a] Calculated [27]

[b] Power input differs from volt-amperes due to non-unity power factor.

Table III. Type IV light source spectral features of hydrogen and strontium at 664°C.

Measured Wavelength (*nm*)	Spectrometer System Irradiation ($\mu W/cm^2 nm$)	Published Emission Data [28] (*nm*)
460.6	0.156	460.73 (Sr I)
487.2	0.00290	487.25 (Sr I), 486.13 (H I)
639.8	0.00813	638.82 (Sr I)
654.7	0.0139	654.68 (Sr I), 656.29 (H I)
689.4	0.0386	689.26 (Sr I)

Table IV. Type IV light source spectral features of hydrogen at 664°C.

Measured Wavelength (nm)	Spectrometer System Irradiation ($\mu W/cm^2 nm$)	Published Emission Data [28] (nm)
485.8	0.0165	486.13 (H I)
518.2	0.00894	
558.7	0.00694	
589.1	0.0174	589.00 (Na I), 589.59 (Na I)
656.7	0.0752	656.29 (H I)

Table V. Type IV light source spectral features of hydrogen and sodium at 335°C.

Measured wavelength (nm)	Spectrometer System Irradiation ($\mu W/cm^2 nm$)	Published emission data [28] (nm)
467.2	0.00400	466.86 (Na I)
486.2	0.0055	486.13 (H I)
498.4	0.0176	498.28 (Na I)
516.1	0.00380	515.34 (Na I)
569.0	0.114	568.82 (Na I)
589.3	0.302	589.00 (Na I), 589.59 (Na I)
615.9	0.0310	616.07 (Na I)
656.0	0.0422	656.29 (H I), 655.24 (Na II)
657.0	0.0421	656.29 (H I)

Table VI. Type IV light source spectral features of hydrogen and magnesium at 449°C.

Measured wavelength (nm)	Spectrometer system irradiation ($\mu W/cm^2 nm$)	Published emission data [28] (nm)
382.6	0.0843	382.93 (Mg I), 383.23 (Mg I)
384.0	0.0643	383.83 (Mg I)
485.2	0.0122	486.13 (H I)
517.3	0.0353	517.27 (Mg I), 518.36 (Mg I)
588.1	0.0167	589.00 (Na I), 589.59 (Na I)
655.8	0.109	656.29 (H I)

Table VII. Type IV light source spectral features of hydrogen and barium at 666°C.

Measured wavelength (nm)	Spectrometer system irradiation ($\mu W/cm^2 nm$)	Published emission data [28] (nm)
456.2	0.0021	455.40 (Ba II)
492.6	0.002	
552.7	8.4×10^{-4}	553.55 (Ba I)
568.4	0.003	568.26 (Na I)
588.8	0.006	589.00 (Na I)
614.7	9.0×10^{-4}	614.17 (Ba II)
655.9	0.002	656.29 (H I)

Table VIII. Type IV light source spectral features of argon, hydrogen, and strontium at 514°C.

Measured wavelength (nm)	Spectrometer system irradiation ($\mu W/cm^2 nm$)	Published emission data [28] (nm)
459.9	0.176	460.73 (Sr I)
639.4	0.004	638.47 (Ar I)
653.9	0.007	653.81 (Ar I)
688.8	0.116	687.84 (Sr I)

Table IX. Type IV light source spectral features of argon and hydrogen at 519°C.

Measured wavelength (nm)	Spectrometer system irradiation $(\mu W/cm^2 nm)$	Published emission data [28] (nm)
486.0	0.032	486.13 (H I)
588.5	0.020	588.86 (Ar I)
656.2	0.176	656.29 (H I)
738.5	0.034	738.40 (Ar I)

Table X. Type IV light source spectral features of argon at 520°C.

Measured wavelength (nm)	Spectrometer system irradiation $(\mu W/cm^2 nm)$	Published emission data [28] (nm)
588.8	0.039	588.86 (Ar I)
655.9	0.046	656.29 (H I)
696.4	0.028	696.54 (Ar I)
706.5	0.028	706.72 (Ar I)
738.5	0.058	738.40 (Ar I)

Table XI. Glow discharge parameters from von Engel [29] and Naidu and Kamaraju [30].

Gas	Minimum starting voltage (V)	Pressure-discharge gap product at minimum starting voltage (cm-torr)
N_2	251	0.67
H_2	273	1.15
Air	327	0.567
CO_2	420	0.51
Ar	137	0.9
He	156	4.0
Hg	520	2
Na	335	0.04

Figure Captions

Figure 1. The experimental set up of a Type I light source comprising a gas cell light source and a VUV spectrometer which was differentially pumped.

Figure 2. The experimental set up of a Type II light source comprising a microwave plasma cell and a VUV spectrometer which was differentially pumped.

Figure 3. Cylindrical stainless steel cell comprising a Type III light source for studies of the broadening of the Balmer α line emitted from gas discharge plasmas of pure hydrogen alone or with strontium or magnesium or a mixture of 10% hydrogen and helium, argon, krypton, or xenon.

Figure 4. Cylindrical stainless steel gas cell comprising a Type IV light source for plasma studies with 1.) hydrogen, argon, or argon-hydrogen mixture alone, 2.) hydrogen with strontium, sodium, magnesium, or barium, and 3.) argon-hydrogen mixture (77/23%) with strontium.

Figure 5. The experimental setup for generating a glow discharge hydrogen plasma and for optically measuring the power balance of the Type IV light source.

Figure 6. The intensity of the Lyman α emission as a function of time from the Type I light source. The gas cell at a cell temperature of 700°C comprised a tungsten filament, a titanium dissociator, vaporized strontium metal, and 300 mtorr hydrogen that was recorded with a CEM.

Figure 7. The VUV spectrum ($90-130\,nm$) of the Type I light source emission recorded at about the point of the maximum Lyman α emission. The gas cell at a cell temperature of 700°C comprised a tungsten filament, a titanium dissociator, vaporized strontium metal, and 300 mtorr hydrogen that was recorded with a CEM.

Figure 8. The VUV spectrum ($80-130\,nm$) of the Type I light source emission recorded at about the point of the maximum Lyman α emission. The gas cell at a cell temperature of 700°C comprised a tungsten filament, vaporized strontium metal, and 300 mtorr argon-hydrogen mixture (97/3%) that was recorded with a PMT and a sodium salicylate scintillator.

Figure 9. The VUV spectrum ($35-67\,nm$) of a strontium rt-plasma Type I light source emission. Line emission corresponding to Sr^{3+} that confirmed the catalyst mechanism was observed at $66.4\,nm$, $41.35\,nm$, and $39.6\,nm$. Sr^{2+} was observed at $56.3\,nm$, $51.4\,nm$, $49.2\,nm$, and $43.7\,nm$

Figure 10. The high resolution visible spectrum ($400-410\,nm$) of a strontium rt-plasma Type I light source emission. Line emission corresponding to Sr^{+} was observed at $407.77\,nm$. Sr was observed at $403.03\,nm$.

Figure 11. The VUV spectrum ($30-170\,nm$) of the cell emission from a Type I light source comprising a gas cell at a cell temperature of 700 °C with a tungsten filament, vaporized strontium metal, and 300 mtorr argon-hydrogen mixture (97/3%) that showed novel catalysts features and spectral lines.

Figure 12. Standard VUV hydrogen emission spectrum ($20-62.5\,nm$) recorded on a Type II light source with the McPherson model 302 (Seya-Namioka type) VUV spectrometer, a PMT, and a sodium salicylate scintillator.

Figure 13. Standard VUV argon emission spectrum ($38-50\,nm$) recorded on a Type II light source with the McPherson 4° grazing incidence EUV spectrometer (Model 248/310G) and a CEM.

Figure 14. The 656.3 nm Balmer α line width recorded with a high resolution ($\pm 0.006\,nm$) visible spectrometer on the Type I light source emission of a hydrogen-strontium rt-plasma. Significant broadening was observed corresponding to an average hydrogen atom temperature of $14\,eV$.

Figure 15. The 656.3 nm Balmer α line width recorded with a high resolution ($\pm 0.006\,nm$) visible spectrometer on the Type I light source emission of a hydrogen-strontium rt-plasma intensified by argon ion catalyst. Significant broadening was observed corresponding to an average hydrogen atom temperature of $24\,eV$.

Figure 16. The superposition of the 656.3 nm Balmer α line width spectra recorded on Type I light source emission of a hydrogen-strontium rt-plasma and a hydrogen-strontium rt-plasma intensified by argon ion catalyst . By comparison to the strontium rt-plasma, significant broadening attributable to argon ion was observed corresponding to an average hydrogen atom temperature of $24\,eV$ versus $14\,eV$.

Figure 17. The 656.3 nm Balmer α line width recorded with a high resolution ($\pm 0.025\,nm$) visible spectrometer on a xenon-hydrogen and a hydrogen gas discharge plasma of a Type III light source. No excessive line broadening was observed corresponding to an average hydrogen atom temperature of $\approx 3\,eV$.

Figure 18. The 656.3 nm Balmer α line width recorded with a high resolution ($\pm 0.025\,nm$) visible spectrometer on a strontium-hydrogen and a hydrogen gas discharge plasma of a Type III light source. Significant broadening was observed corresponding to an average hydrogen atom temperature of $23-25\,eV$.

Figure 19. The 656.3 nm Balmer α line width recorded with a high resolution ($\pm 0.025\,nm$) visible spectrometer on a strontium-helium-hydrogen and a hydrogen gas discharge plasma of a Type III light source. Significant broadening was observed corresponding to an average hydrogen atom temperature of $40-45\,eV$.

Figure 20. The 656.3 nm Balmer α line width recorded with a high resolution ($\pm 0.025\,nm$) visible spectrometer on a strontium-argon-hydrogen, strontium-argon, and a hydrogen gas discharge plasma of a Type III light source. Significant broadening was observed corresponding to an average hydrogen atom temperature of $35-40\,eV$.

Figure 21. The count rate and the spectrometer system irradiation of a Type IV light source with a mixture of hydrogen and strontium vapor at 664°C.

Figure 22. The spectrometer system irradiation for a hydrogen discharge of a Type IV light source at a cell temperature of 664°C and a hydrogen pressure of 1 torr.

Figure 23a-c. The spectrometer system irradiation of a Type IV light source with a mixture of hydrogen and sodium vapor at 335, 516, and 664°C.

Figure 24a-c. The spectrometer system irradiation of a Type IV light source with a mixture of hydrogen and magnesium vapor at 449, 582, and 654°C.

Figure 25. The spectrometer system irradiation of a Type IV light source with a mixture of hydrogen and barium vapor at 666°C.

Figure 26. The spectrometer system irradiation of a Type IV light source with a mixture of argon-hydrogen and strontium vapor at 514°C.

Figure 27. The spectrometer system irradiation of a Type IV light source with a mixture of argon and hydrogen at 519°C.

Figure 28. The spectrometer system irradiation of a Type IV light source with an argon discharge at a cell temperature of 520°C and argon pressure of 1 torr.

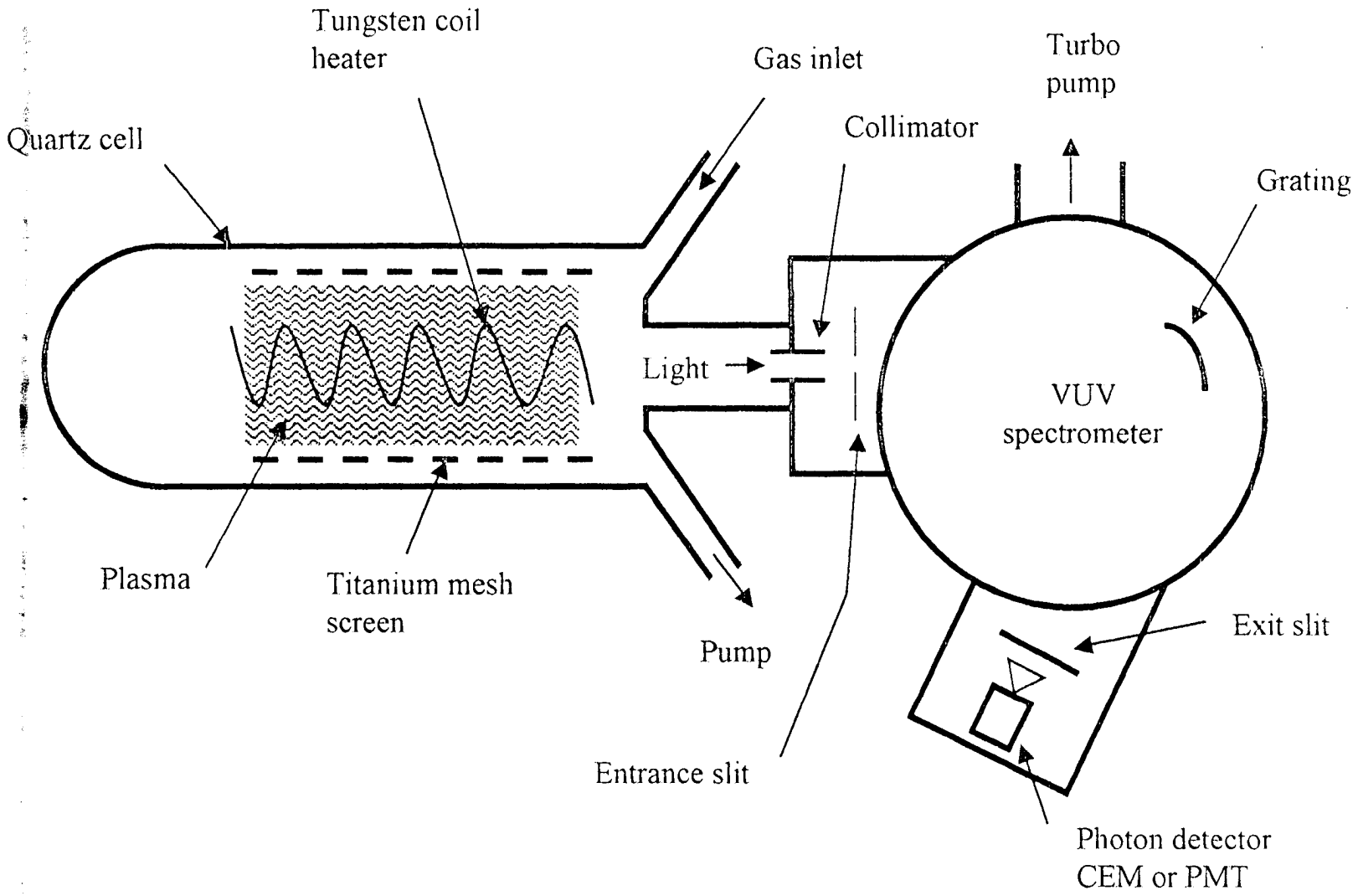
Tungsten coil
heater
Gas inlet
Turbo
pump
Quartz cell
Collimator
Grating
Light
VUV
spectrometer
Plasma
Titanium mesh
screen
Pump
Exit slit
Entrance slit
Photon detector
CEM or PMT

Fig. 1

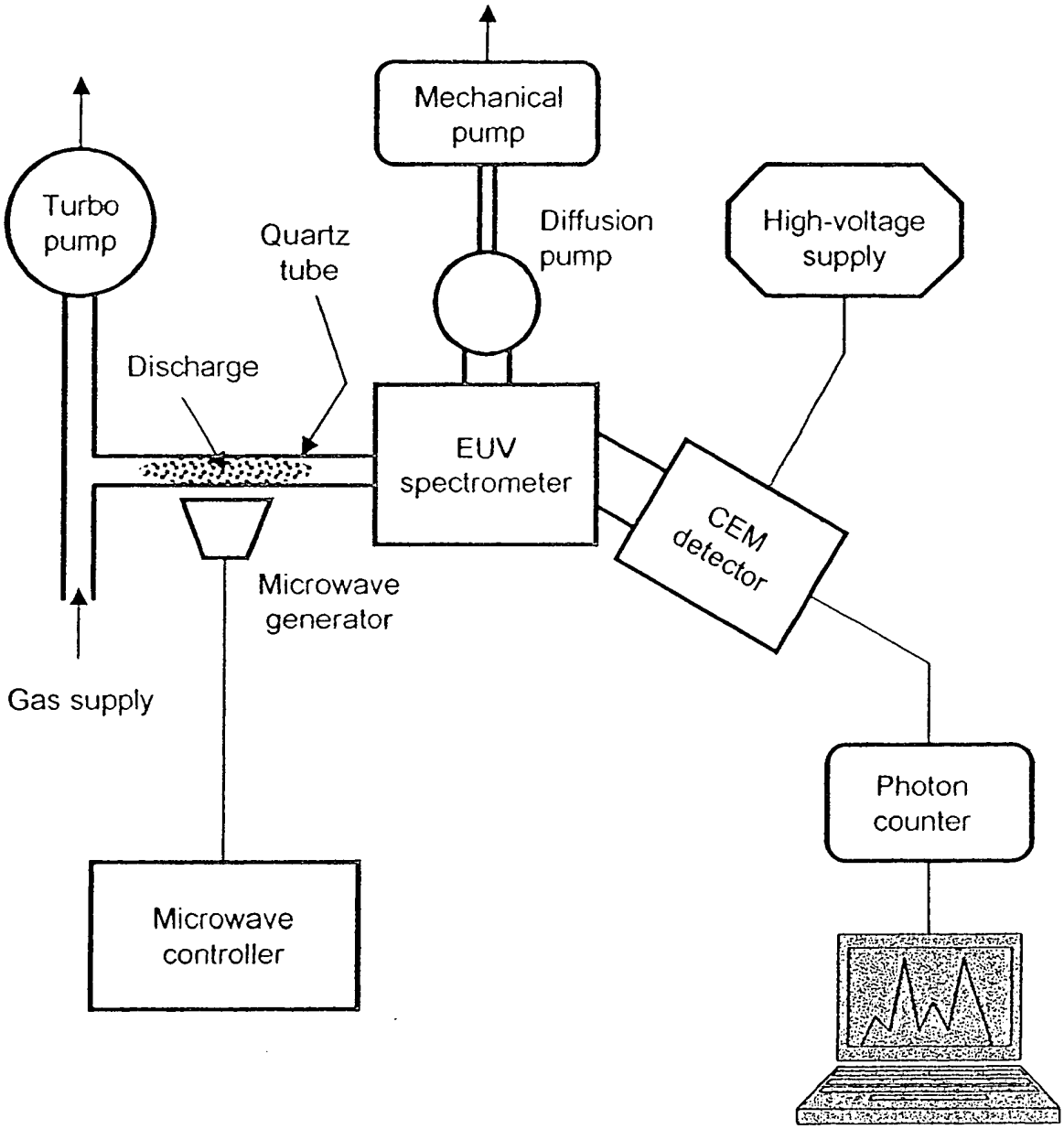
Mechanical pump
Turbo pump
Quartz tube
Diffusion pump
High-voltage supply
Discharge
EUV spectrometer
CEM detector
Microwave generator
Gas supply
Photon counter
Microwave controller

Fig. 2

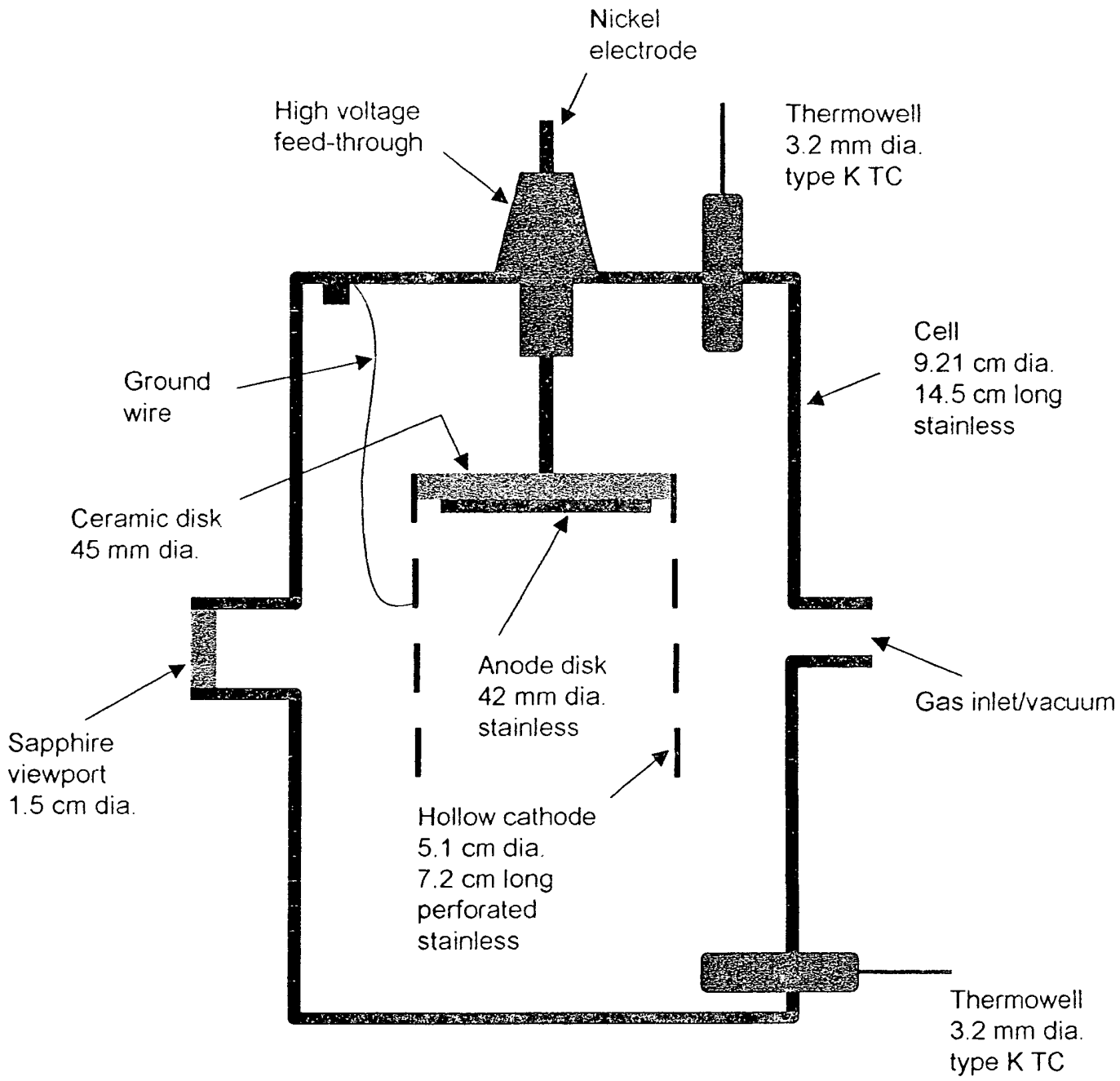
Nickel electrode
High voltage feed-through
Thermowell 3.2 mm dia. type K TC
Cell 9.21 cm dia. 14.5 cm long stainless
Ground wire
Ceramic disk 45 mm dia.
Anode disk 42 mm dia. stainless
Gas inlet/vacuum
Sapphire viewport 1.5 cm dia.
Hollow cathode 5.1 cm dia. 7.2 cm long perforated stainless
Thermowell 3.2 mm dia. type K TC

Fig. 3

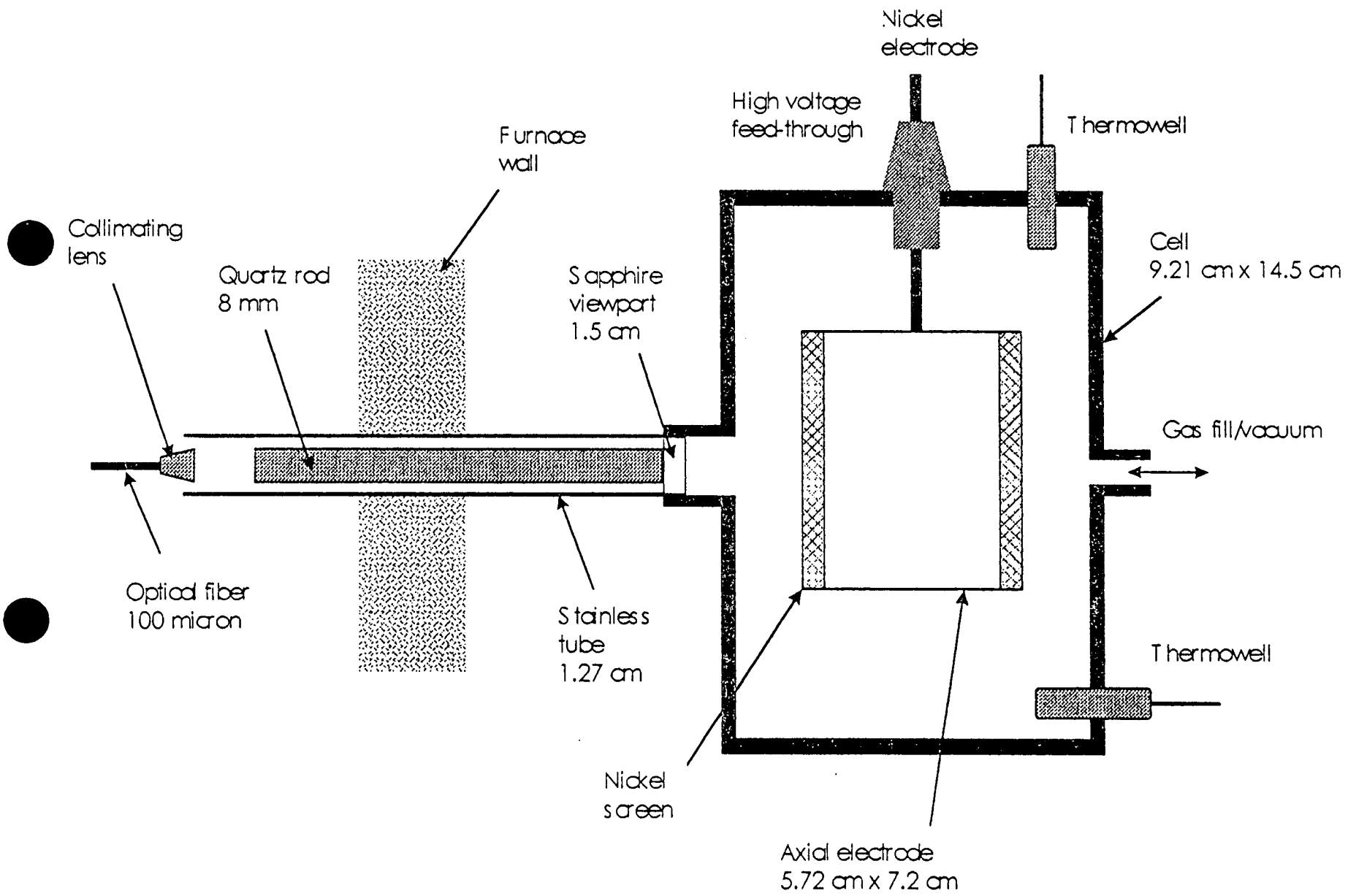
Nickel
electrode
High voltage
feed-through
Thermowell
Furnace
wall
Collimating
lens
Quartz rod
8 mm
Sapphire
viewport
1.5 cm
Cell
9.21 cm x 14.5 cm
Gas fill/vacuum
Optical fiber
100 micron
Stainless
tube
1.27 cm
Thermowell
Nickel
screen
Axial electrode
5.72 cm x 7.2 cm

Fig. 4

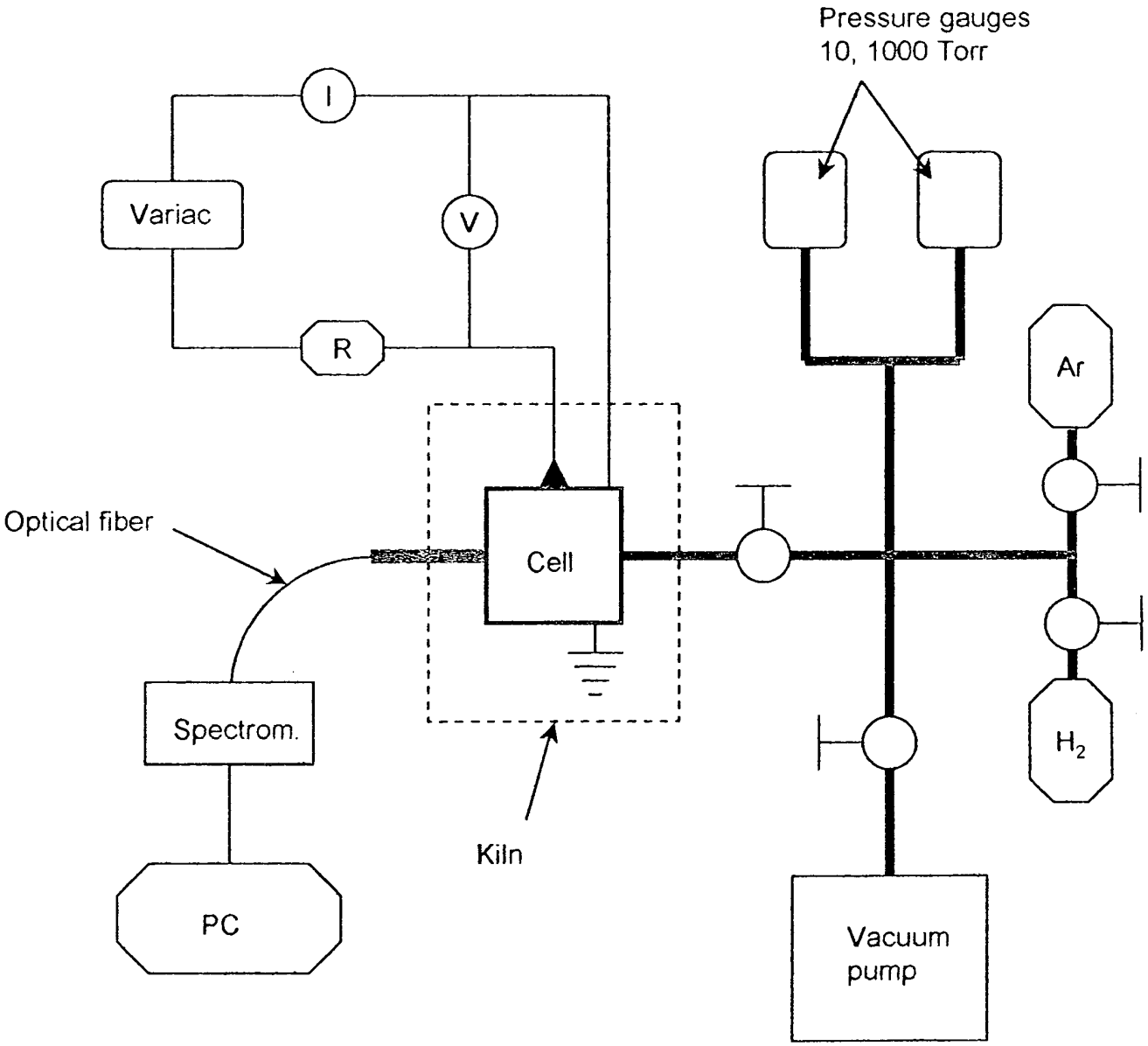
Pressure gauges
10, 1000 Torr
I
Variac
V
R
Ar
Optical fiber
Cell
Spectrom.
Kiln
H_2
PC
Vacuum
pump

Fig. 5

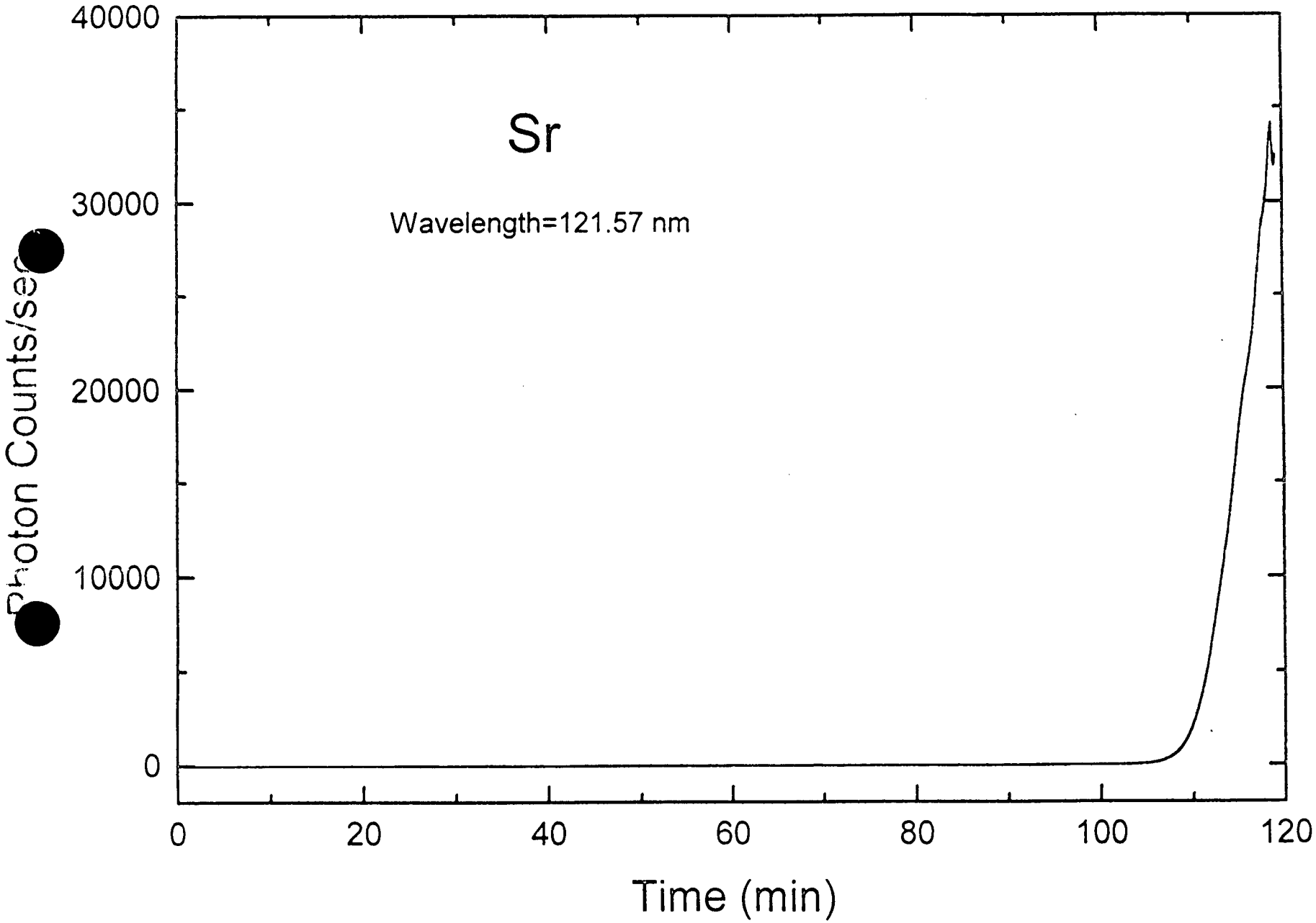
Sr
Wavelength=121.57 nm
Photon Counts/sec
40000
30000
20000
10000
0
0
20
40
60
80
100
120
Time (min)

Fig. 6

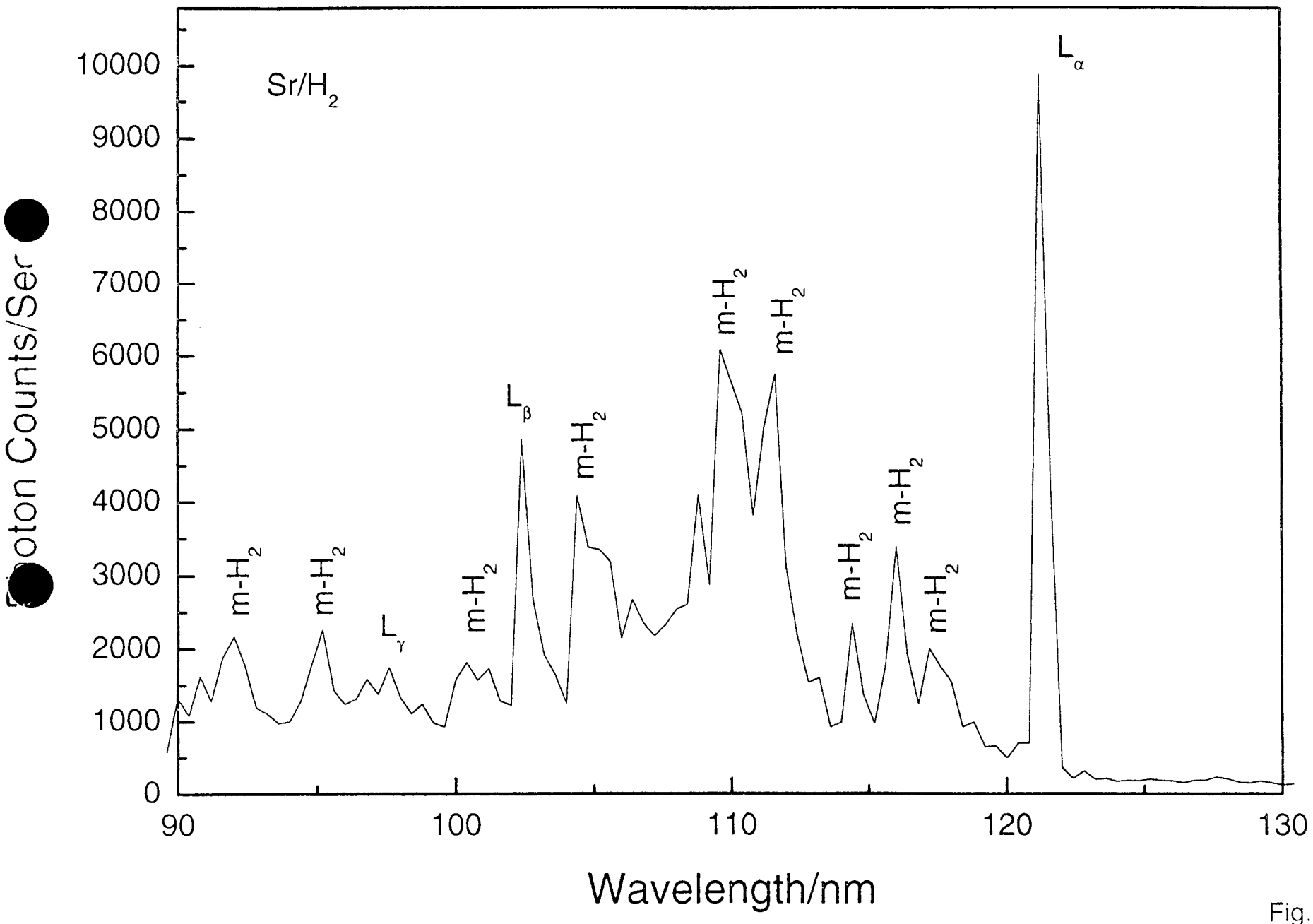
Sr/H2
Photon Counts/Ser
Wavelength/nm
10000
9000
8000
7000
6000
5000
4000
3000
2000
1000
0
90
100
110
120
130
m-H2
Lγ
Lβ
Lα

Fig. 7

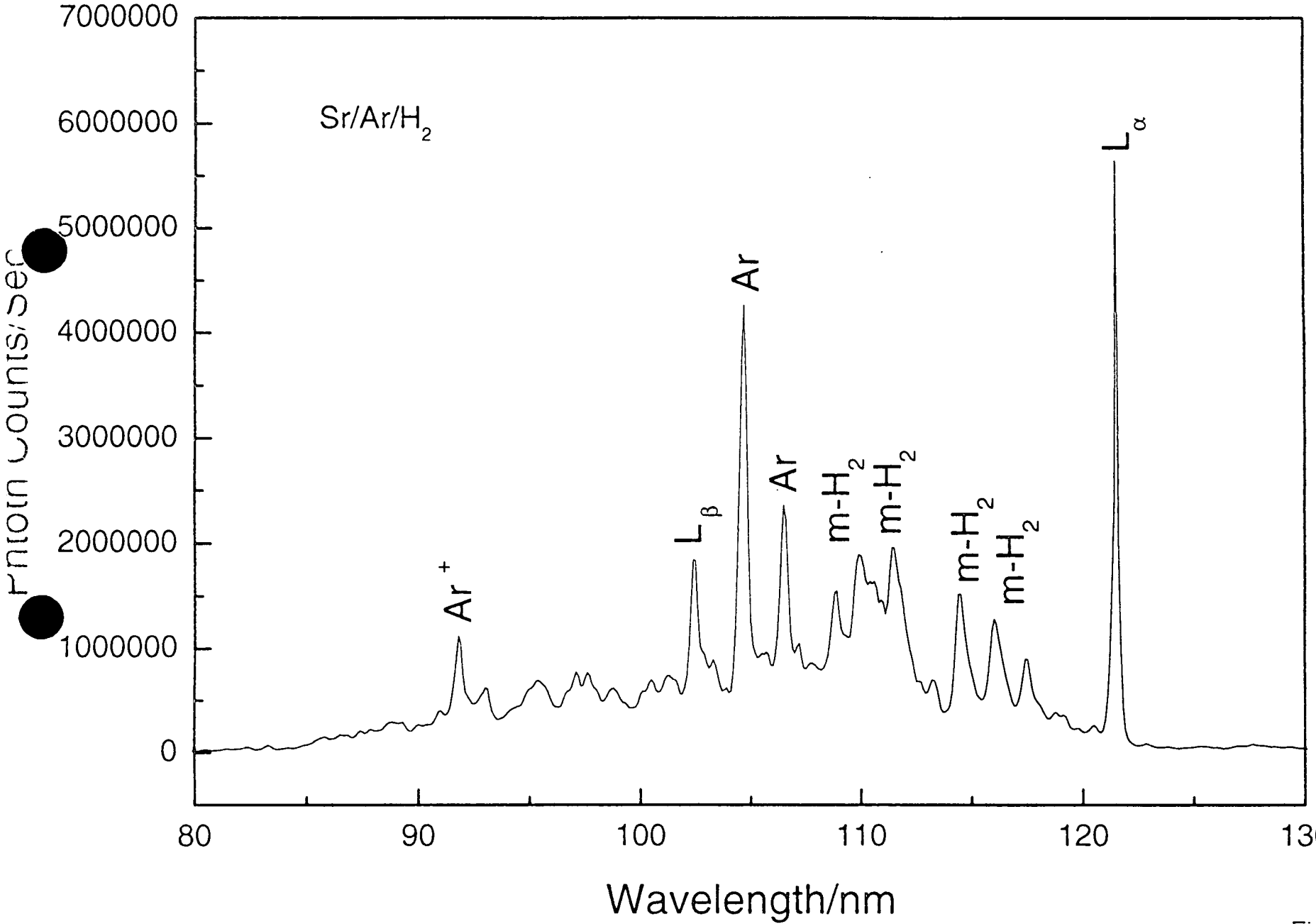
7000000
6000000
5000000
4000000
3000000
2000000
1000000
0
Photon Counts/sec
Sr/Ar/H2
Ar+
Lβ
Ar
Ar
m-H2
m-H2
m-H2
m-H2
Lα
80
90
100
110
120
130
Wavelength/nm

Fig. 8

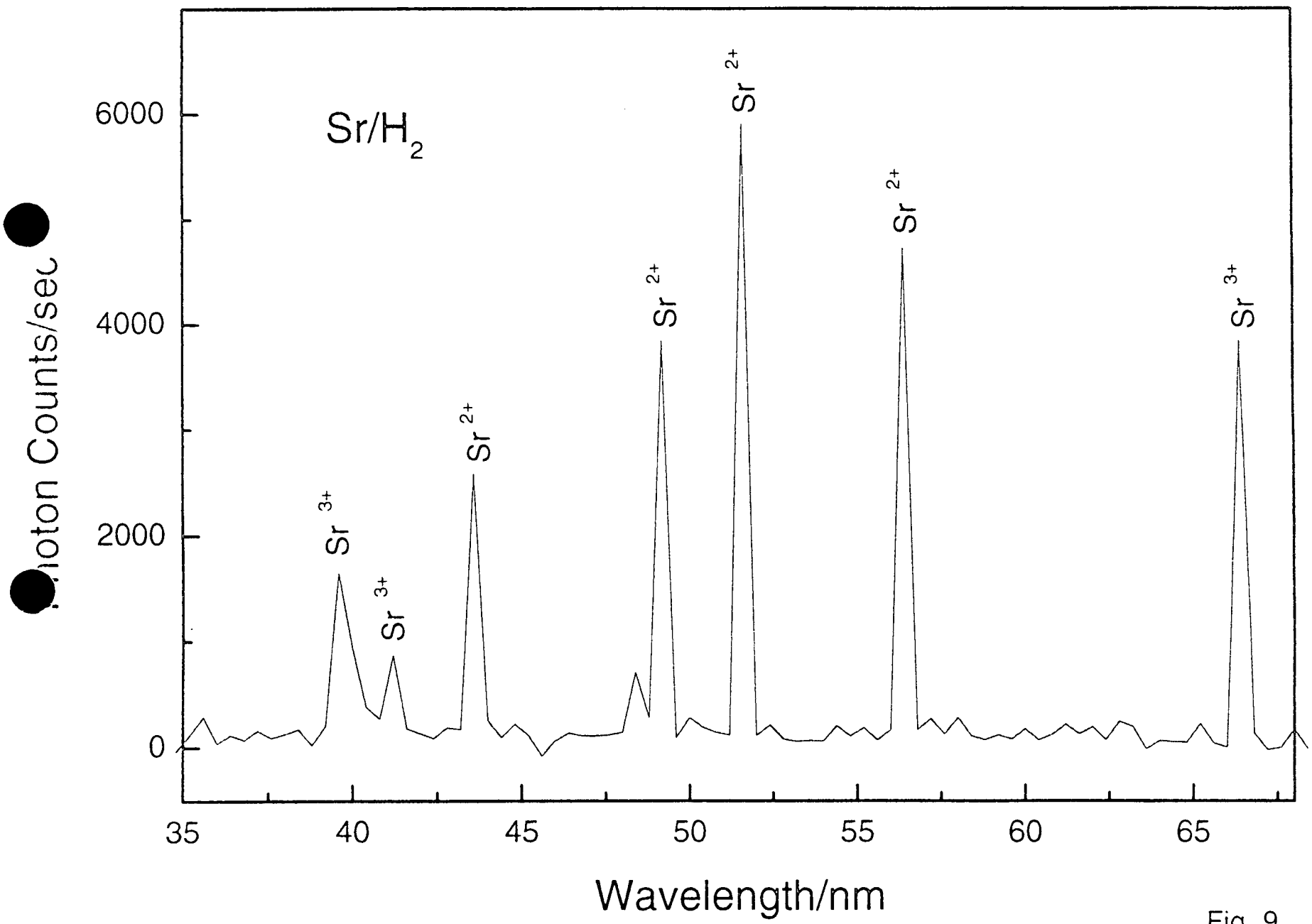
Sr/H2
6000
4000
2000
0
Photon Counts/sec
Sr 3+
Sr 3+
Sr 2+
Sr 2+
Sr 2+
Sr 2+
Sr 3+
35
40
45
50
55
60
65
Wavelength/nm

Fig. 9

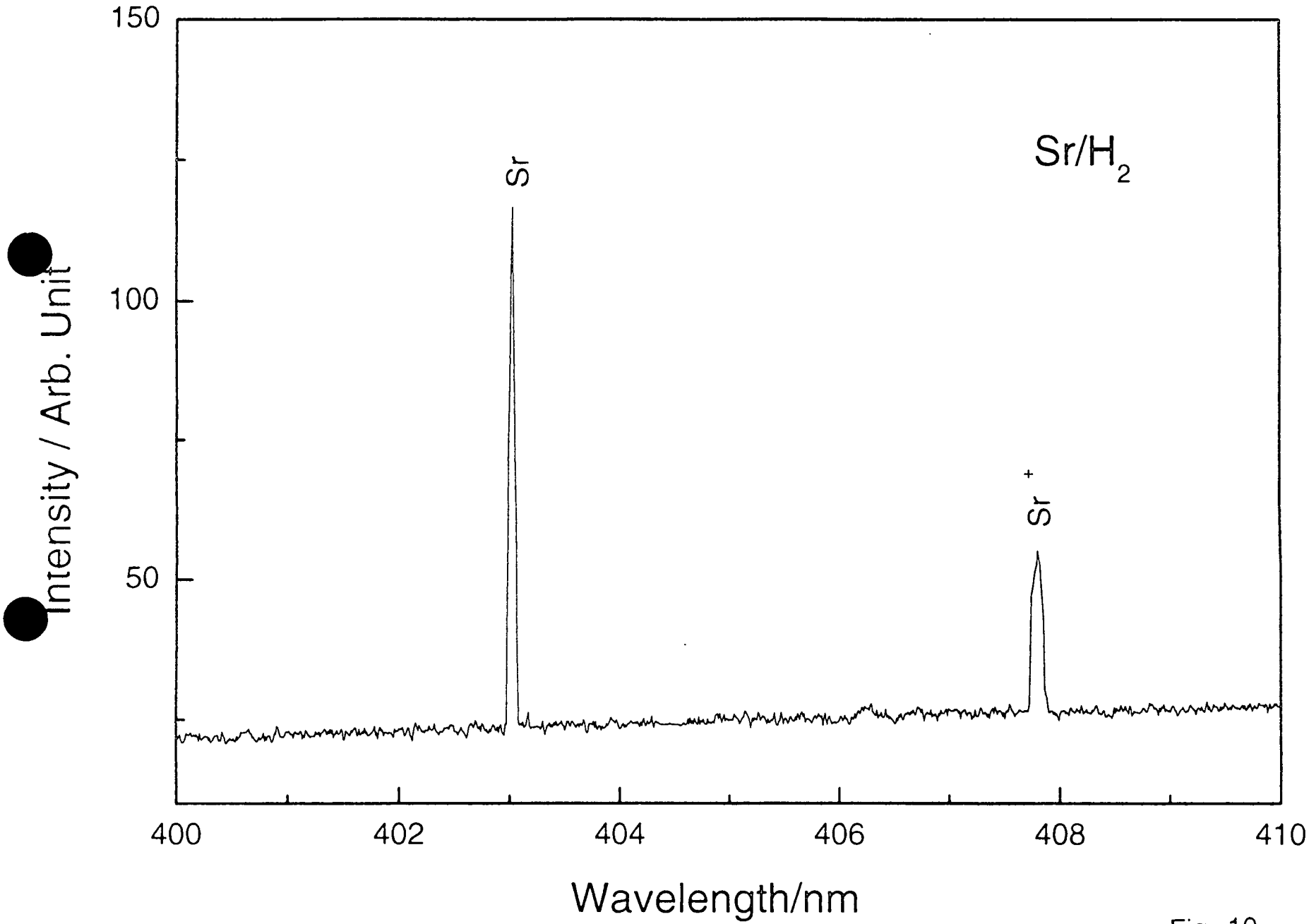
150
100
50
Intensity / Arb. Unit
Sr
Sr/H2
Sr+
400
402
404
406
408
410
Wavelength/nm

Fig. 10

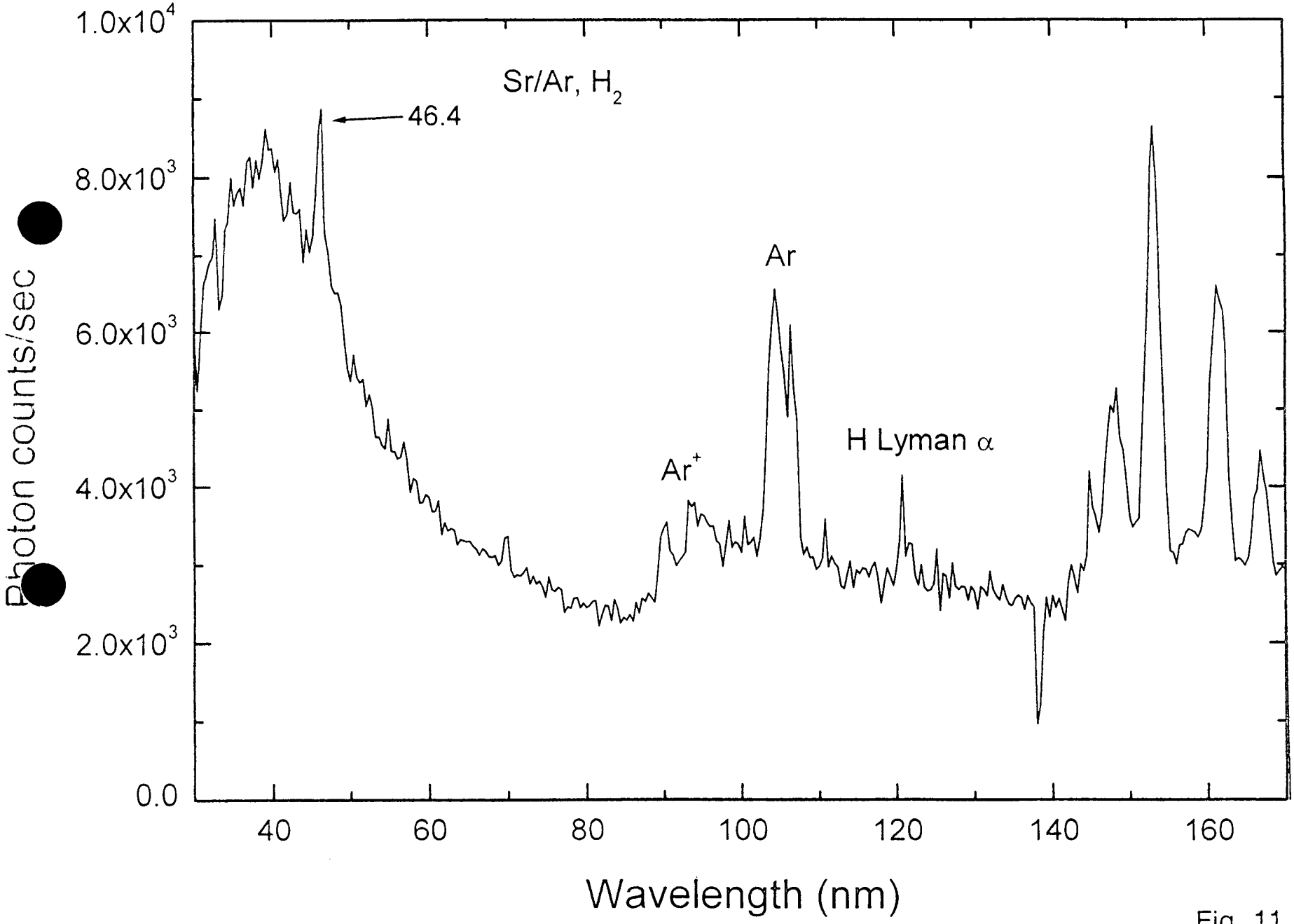
1.0x10^4
8.0x10^3
6.0x10^3
4.0x10^3
2.0x10^3
0.0
Photon counts/sec
Sr/Ar, H2
46.4
Ar+
Ar
H Lyman α
40
60
80
100
120
140
160
Wavelength (nm)

Fig. 11

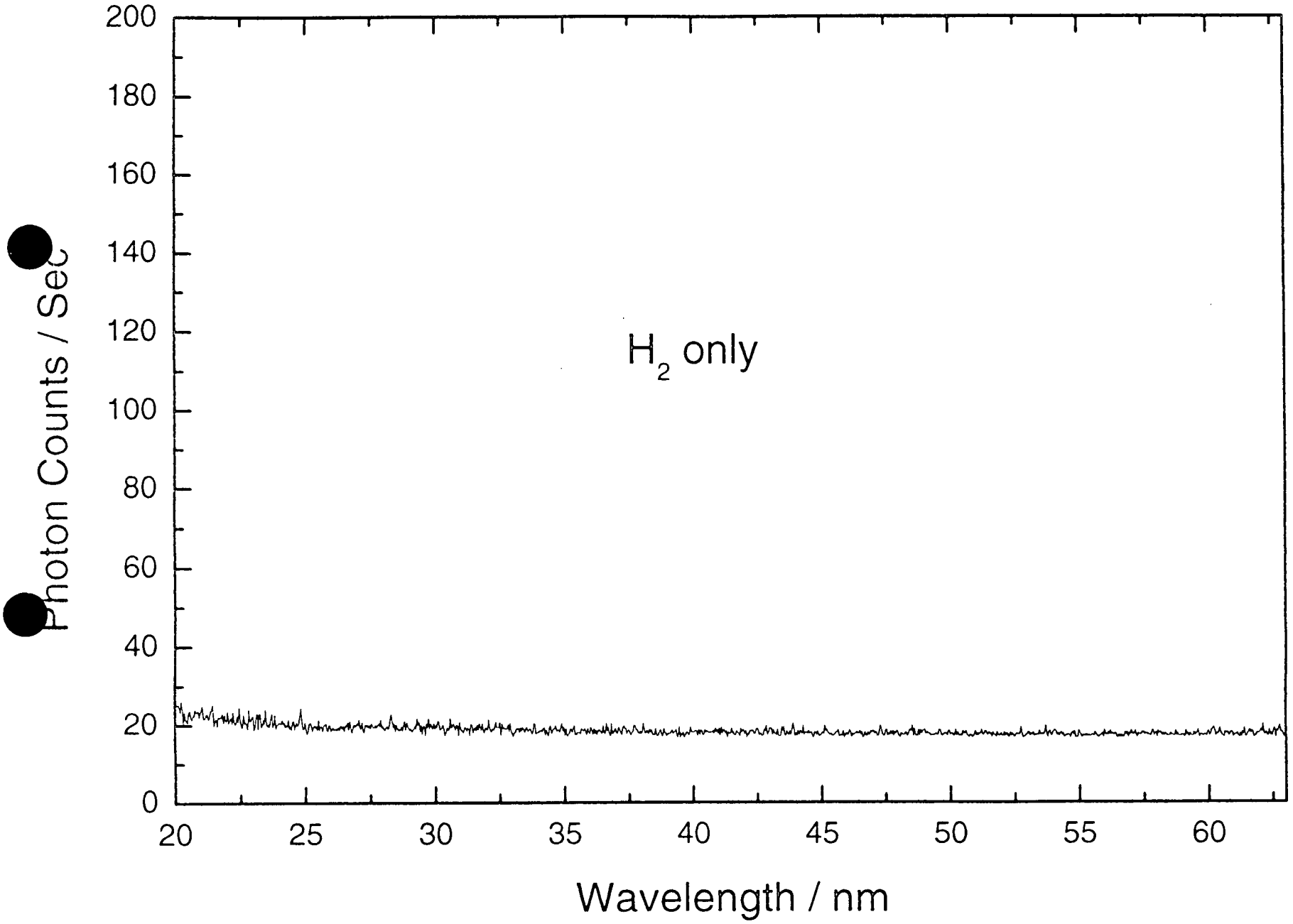
200
180
160
140
120
100
80
60
40
20
0
Photon Counts / Sec
H_2 only
20
25
30
35
40
45
50
55
60
Wavelength / nm

Fig. 12

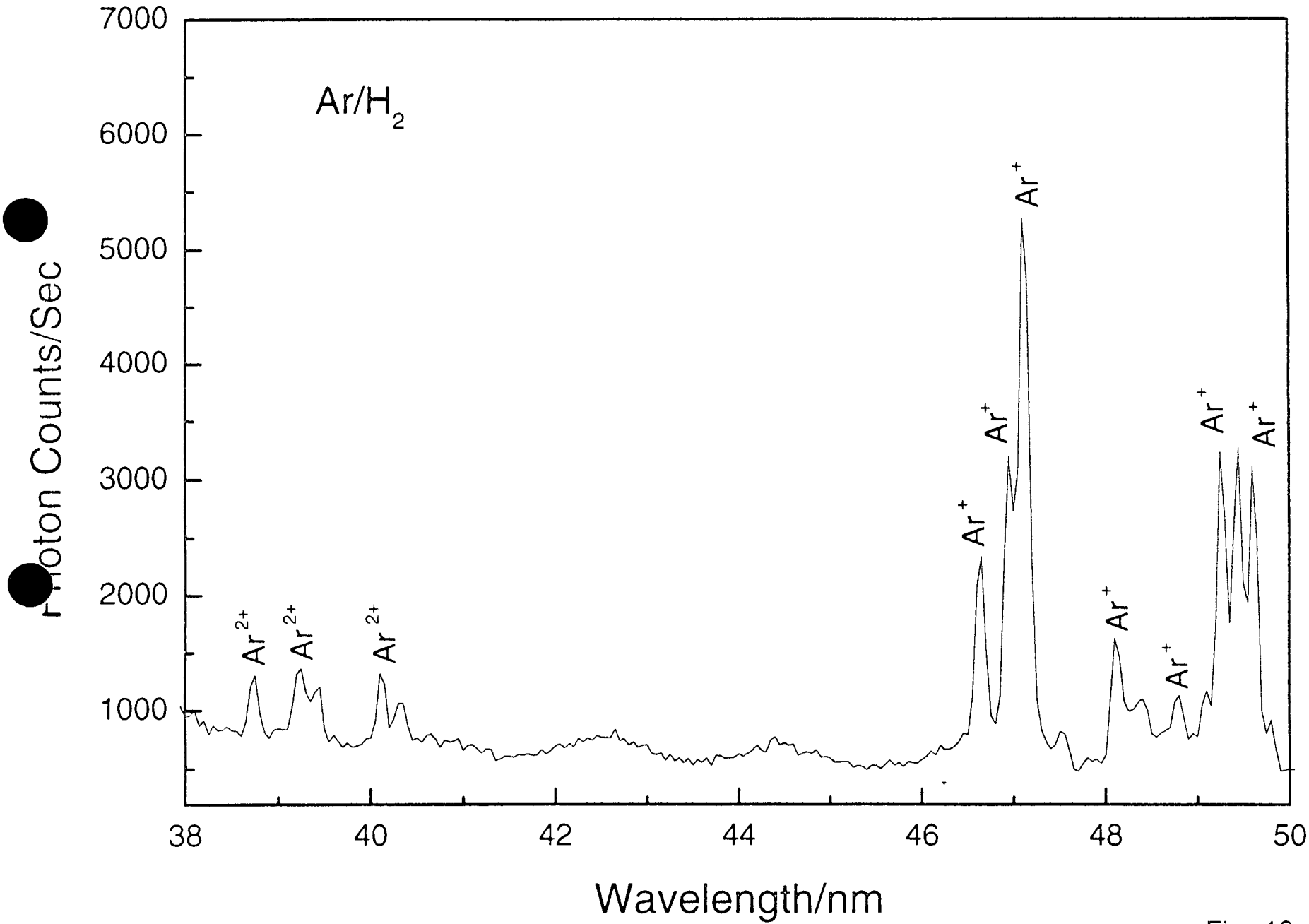
Ar/H2
Photon Counts/Sec
Wavelength/nm
7000
6000
5000
4000
3000
2000
1000
38
40
42
44
46
48
50
Ar2+
Ar2+
Ar2+
Ar+
Ar+
Ar+
Ar+
Ar+
Ar+
Ar+

Fig. 13

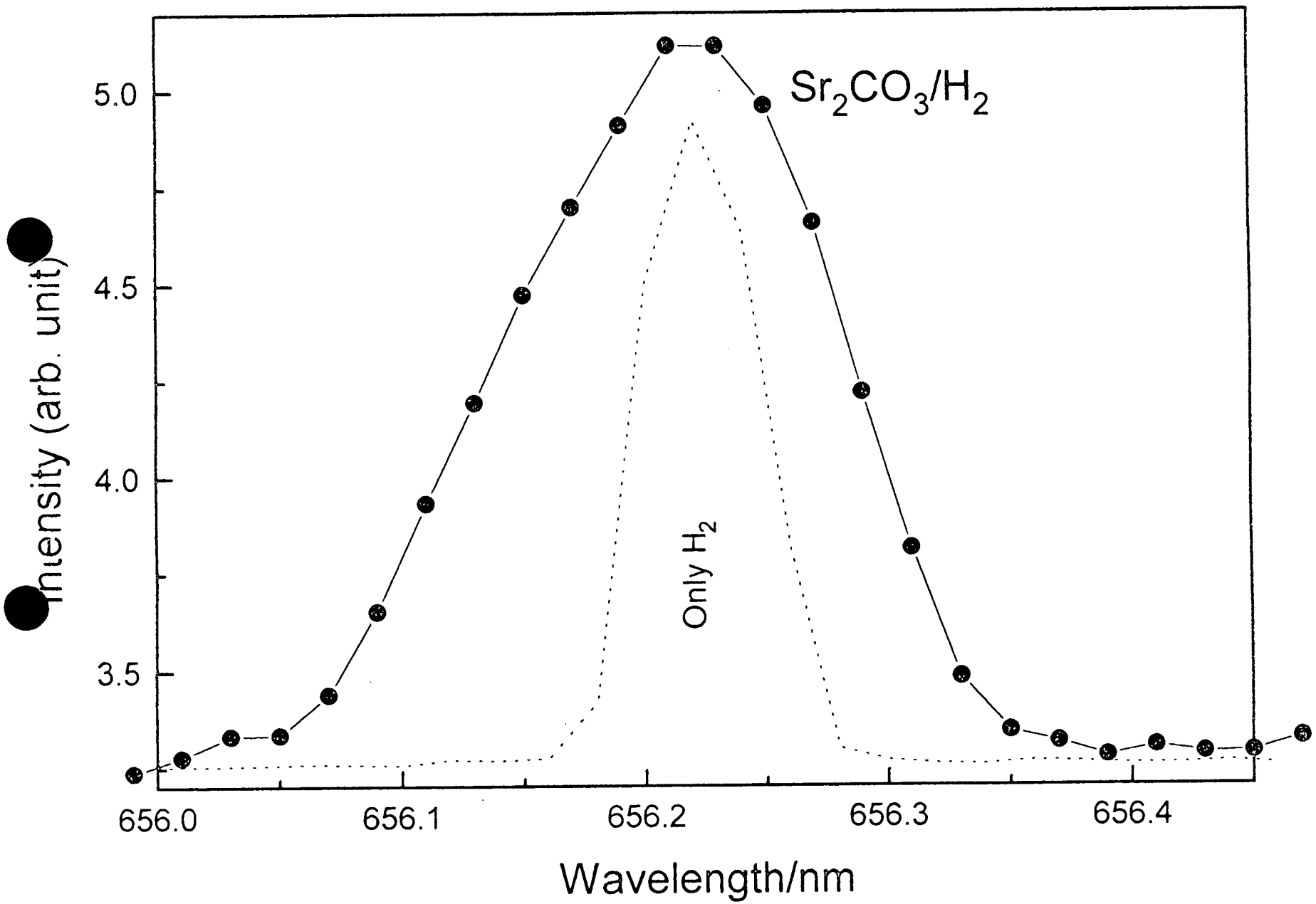
Intensity (arb. unit)
5.0
4.5
4.0
3.5
656.0
656.1
656.2
656.3
656.4
Wavelength/nm
Sr_2CO_3/H_2
Only H_2

Fig. 14

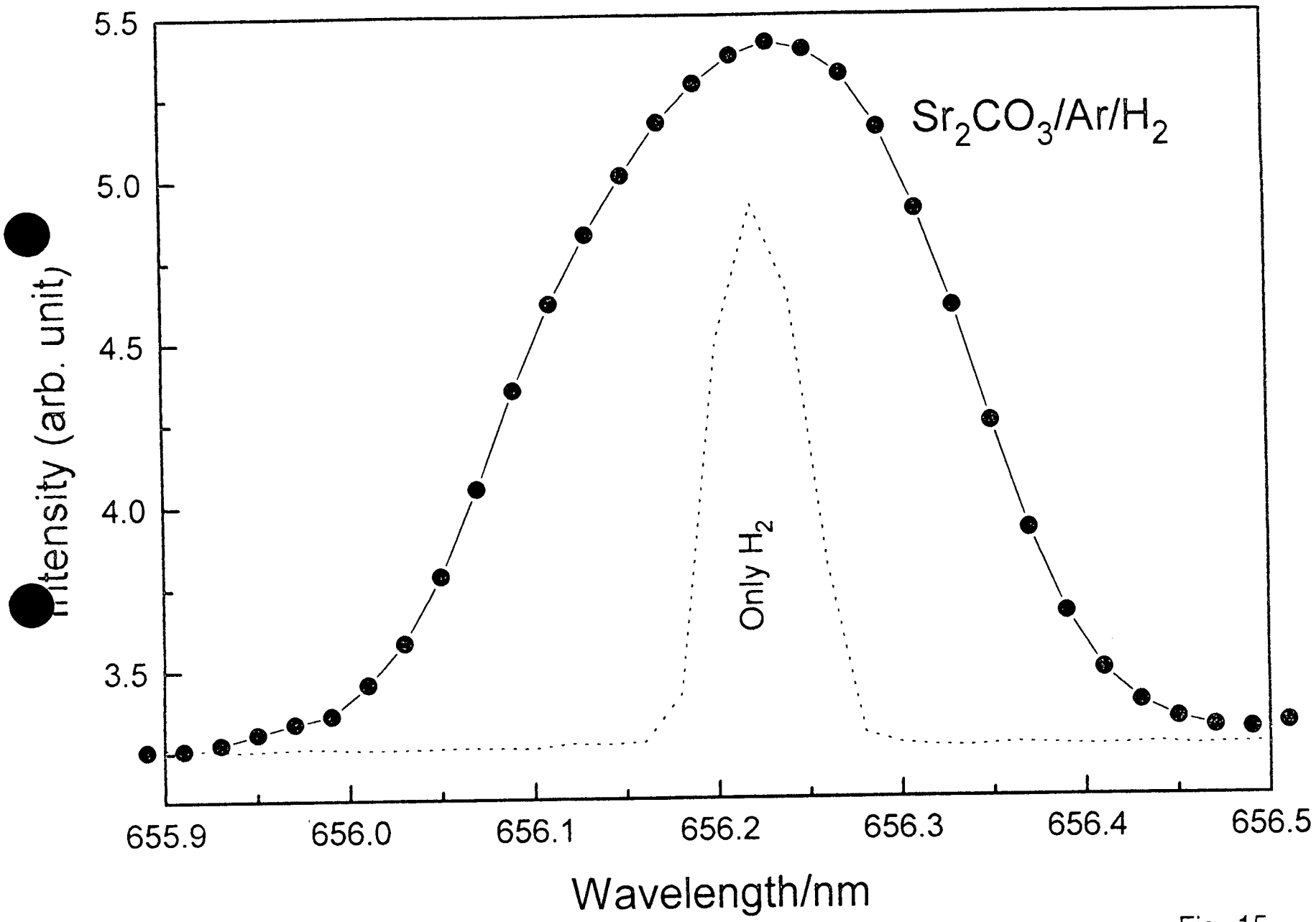
5.5
5.0
4.5
4.0
3.5
Intensity (arb. unit)
$Sr_2CO_3/Ar/H_2$
Only H_2
655.9
656.0
656.1
656.2
656.3
656.4
656.5
Wavelength/nm

Fig. 15

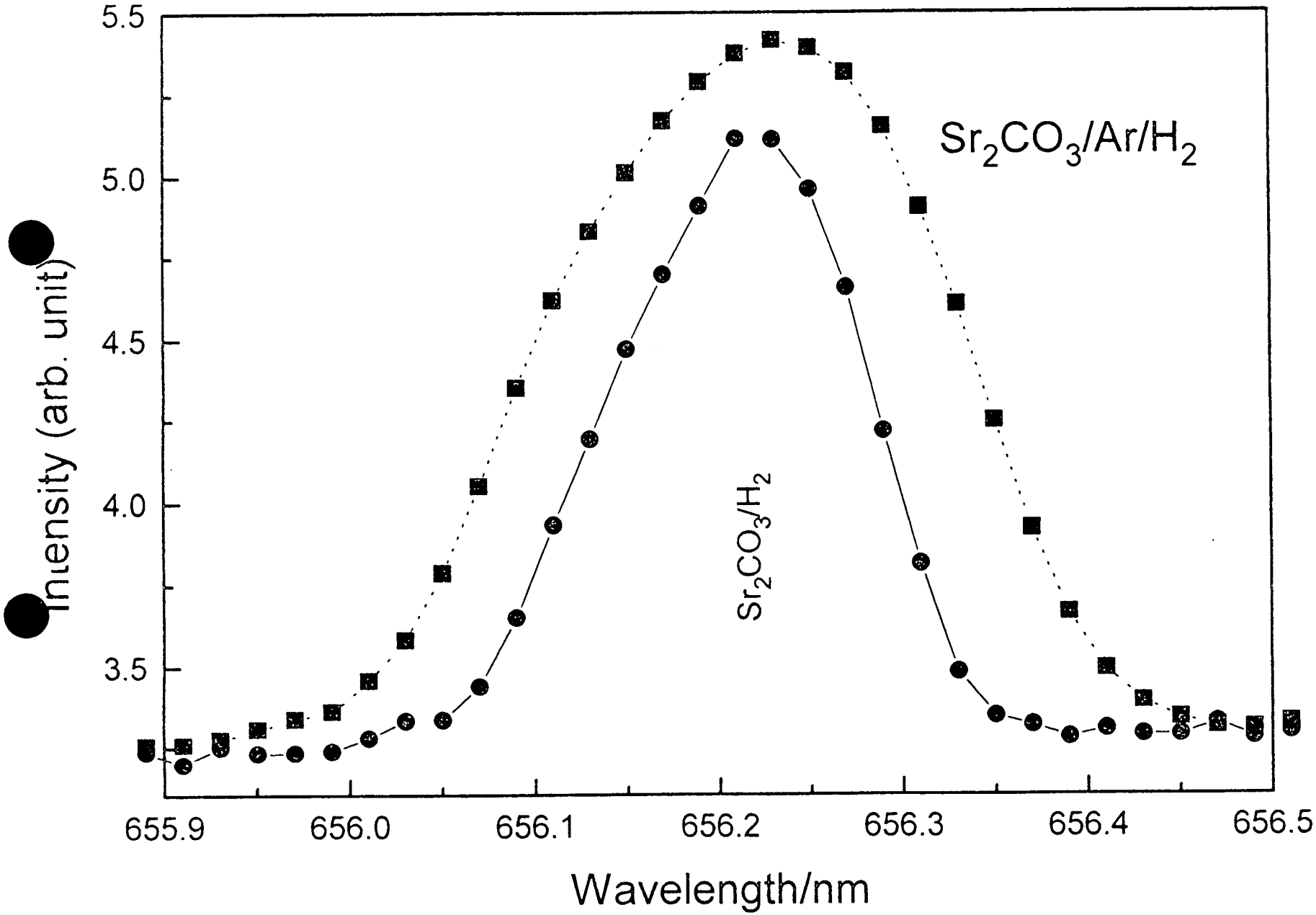
5.5
5.0
4.5
4.0
3.5
Intensity (arb. unit)
$Sr_2CO_3/Ar/H_2$
Sr_2CO_3/H_2
655.9
656.0
656.1
656.2
656.3
656.4
656.5
Wavelength/nm

Fig. 16

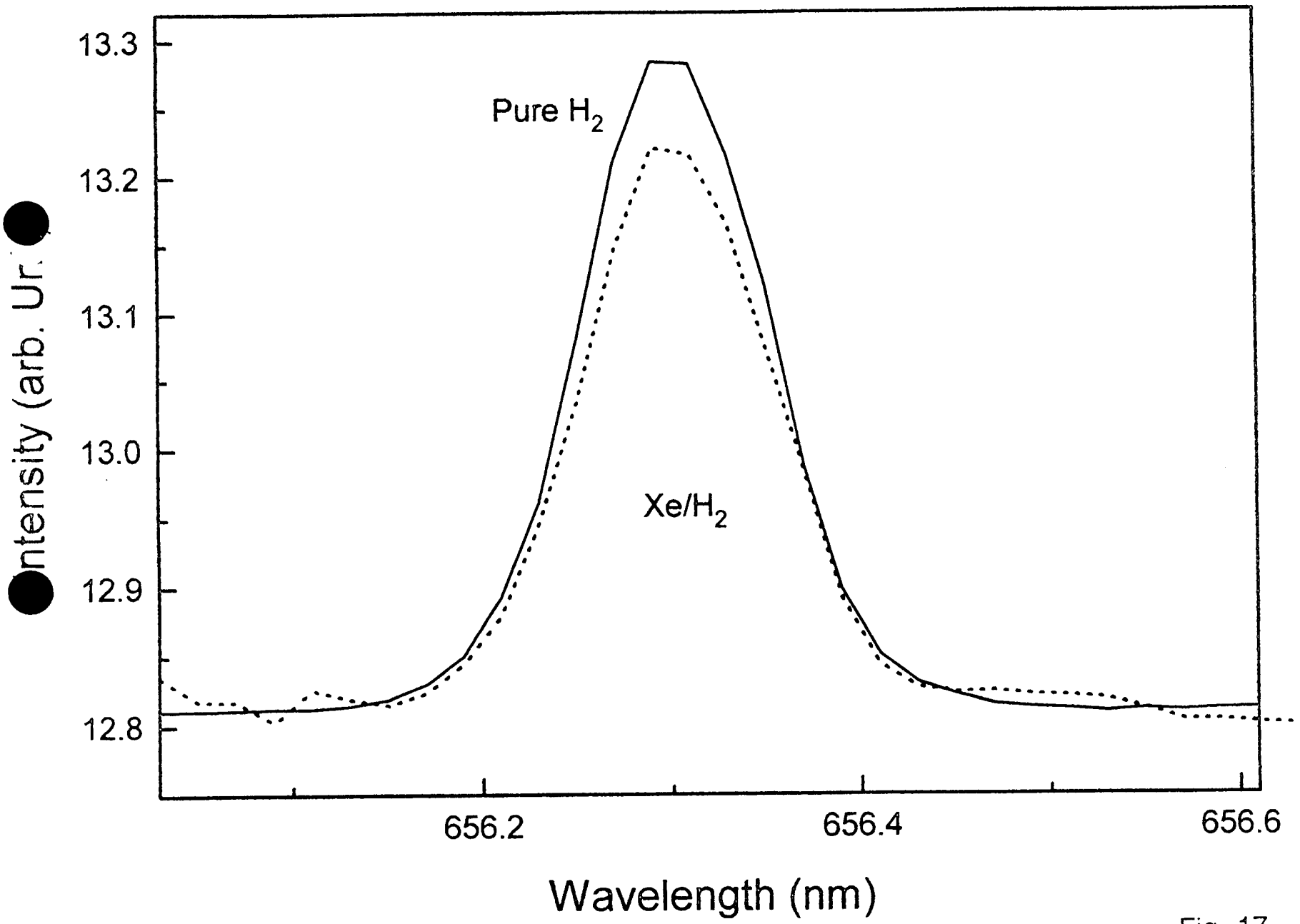
13.3
13.2
13.1
13.0
12.9
12.8
Intensity (arb. Ur
Pure H_2
Xe/H_2
656.2
656.4
656.6
Wavelength (nm)

Fig. 17

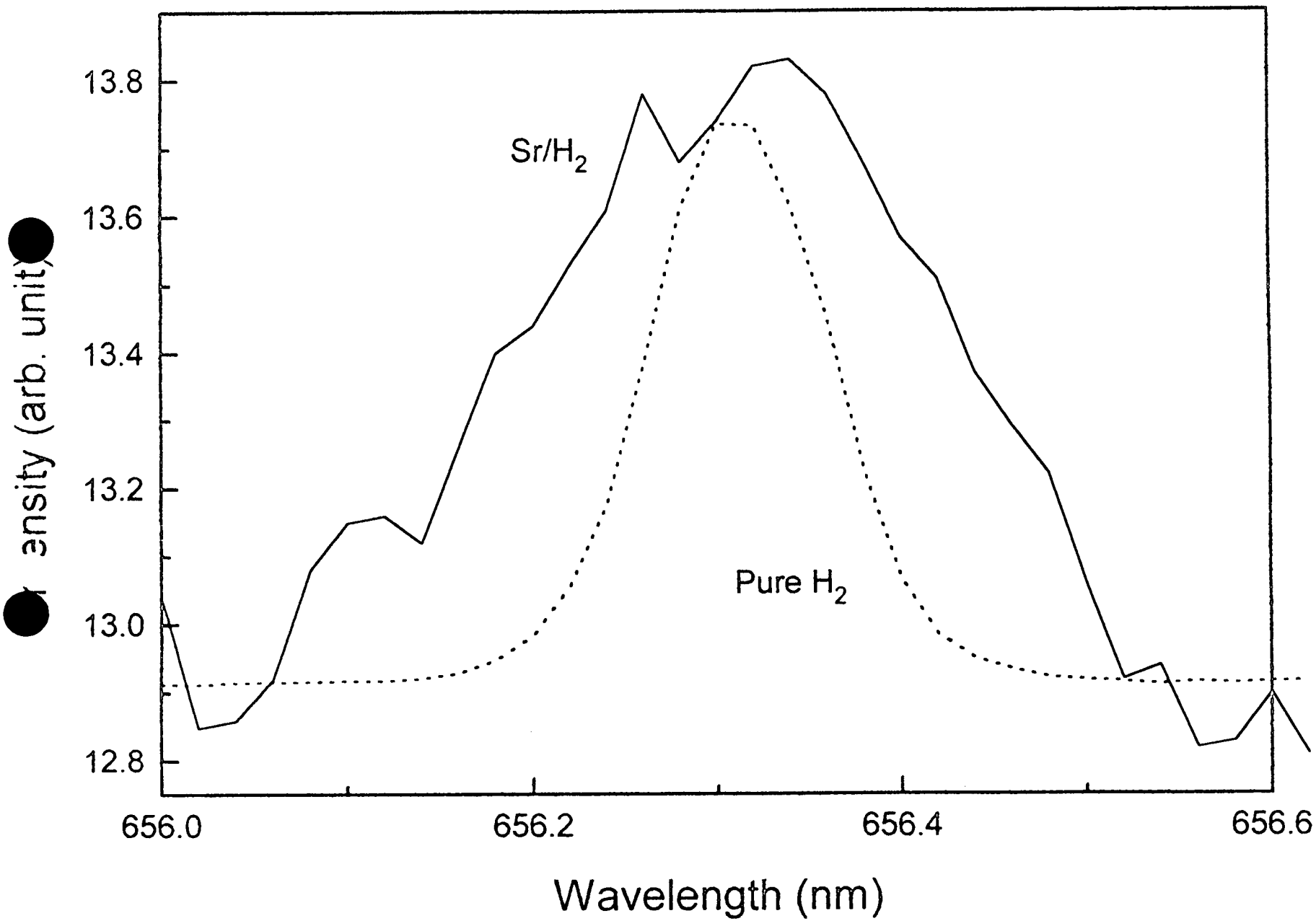
13.8
13.6
13.4
13.2
13.0
12.8
Sr/H2
Pure H2
656.0
656.2
656.4
656.6
Wavelength (nm)

Fig. 18

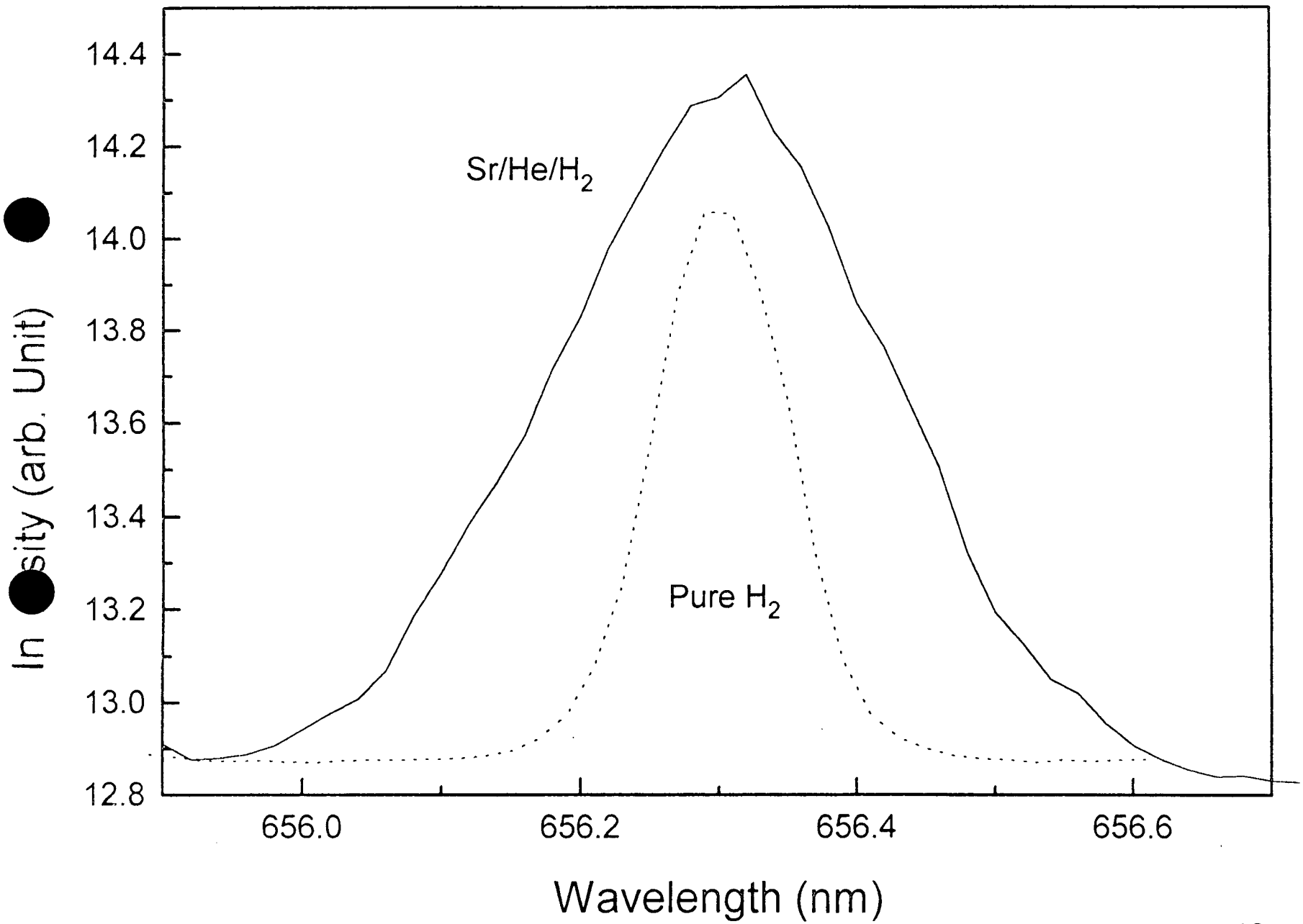
14.4
14.2
14.0
13.8
13.6
13.4
13.2
13.0
12.8
Sr/He/H2
Pure H2
656.0
656.2
656.4
656.6
Wavelength (nm)

Fig. 19

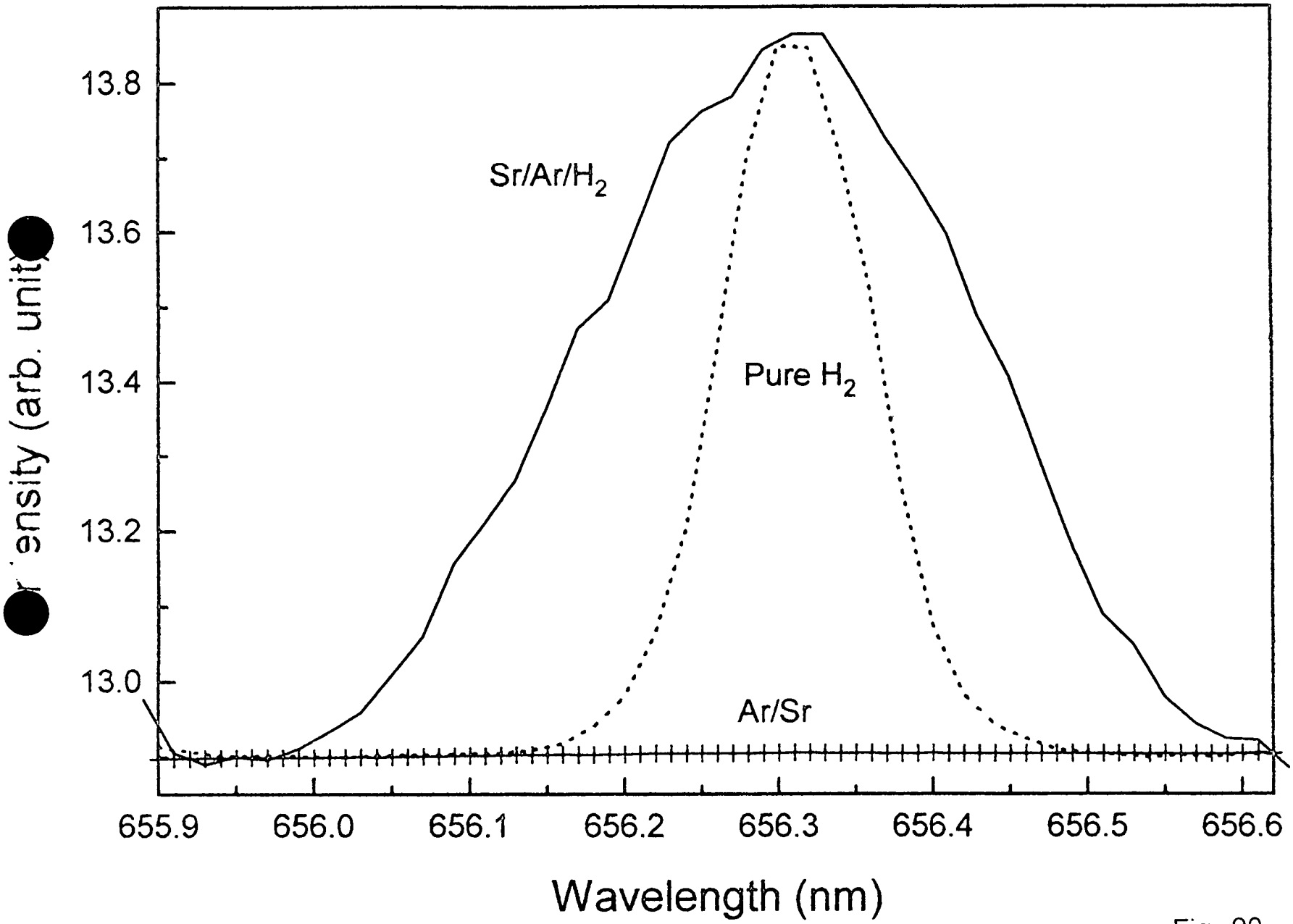
13.8
13.6
13.4
13.2
13.0
Sr/Ar/H2
Pure H2
Ar/Sr
655.9
656.0
656.1
656.2
656.3
656.4
656.5
656.6
Wavelength (nm)

Fig. 20

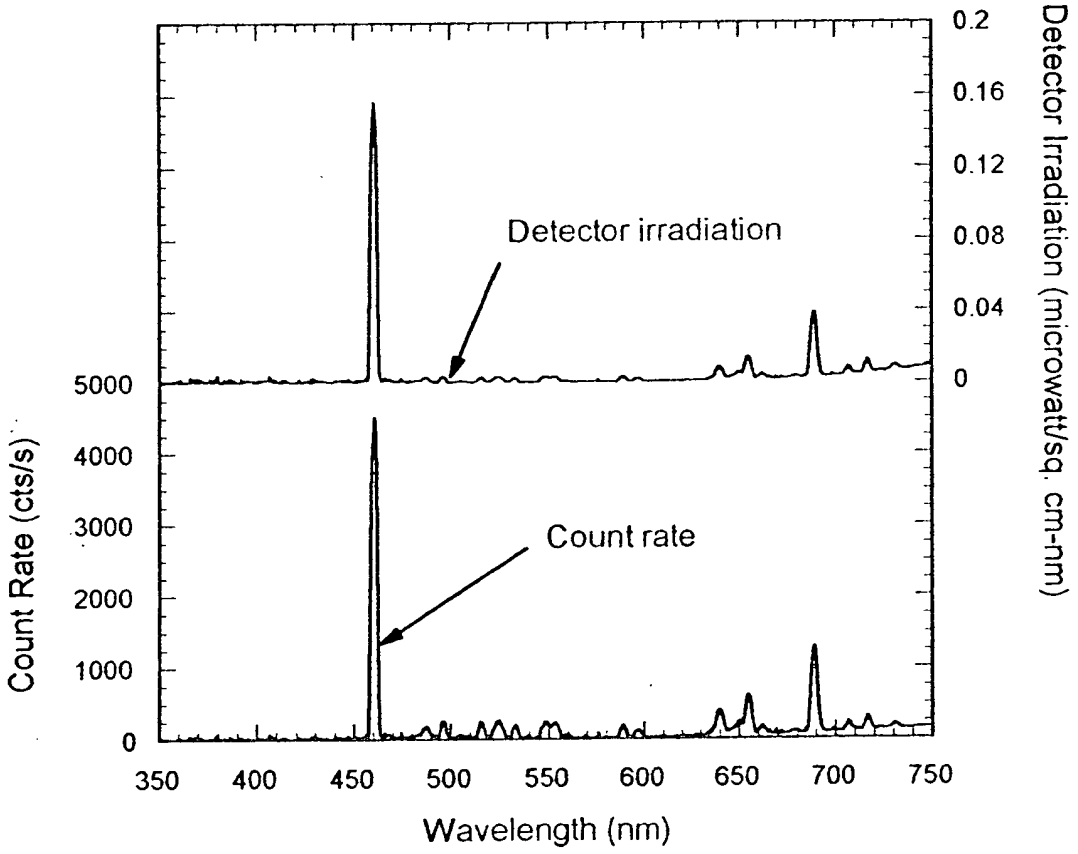
Detector irradiation
Count rate
Count Rate (cts/s)
Detector Irradiation (microwatt/sq. cm-nm)
Wavelength (nm)
0
1000
2000
3000
4000
5000
0
0.04
0.08
0.12
0.16
0.2
350
400
450
500
550
600
650
700
750

Fig. 21

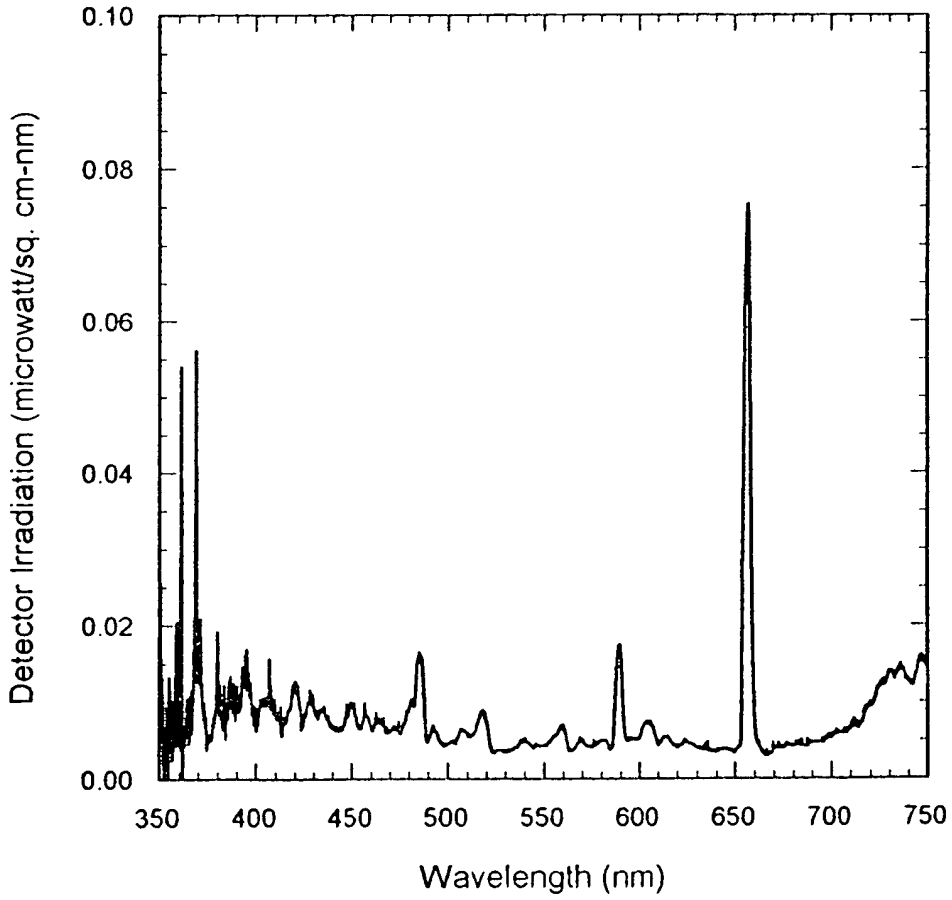
0.10
0.08
0.06
0.04
0.02
0.00
Detector Irradiation (microwatt/sq. cm-nm)
350
400
450
500
550
600
650
700
750
Wavelength (nm)

Fig. 22

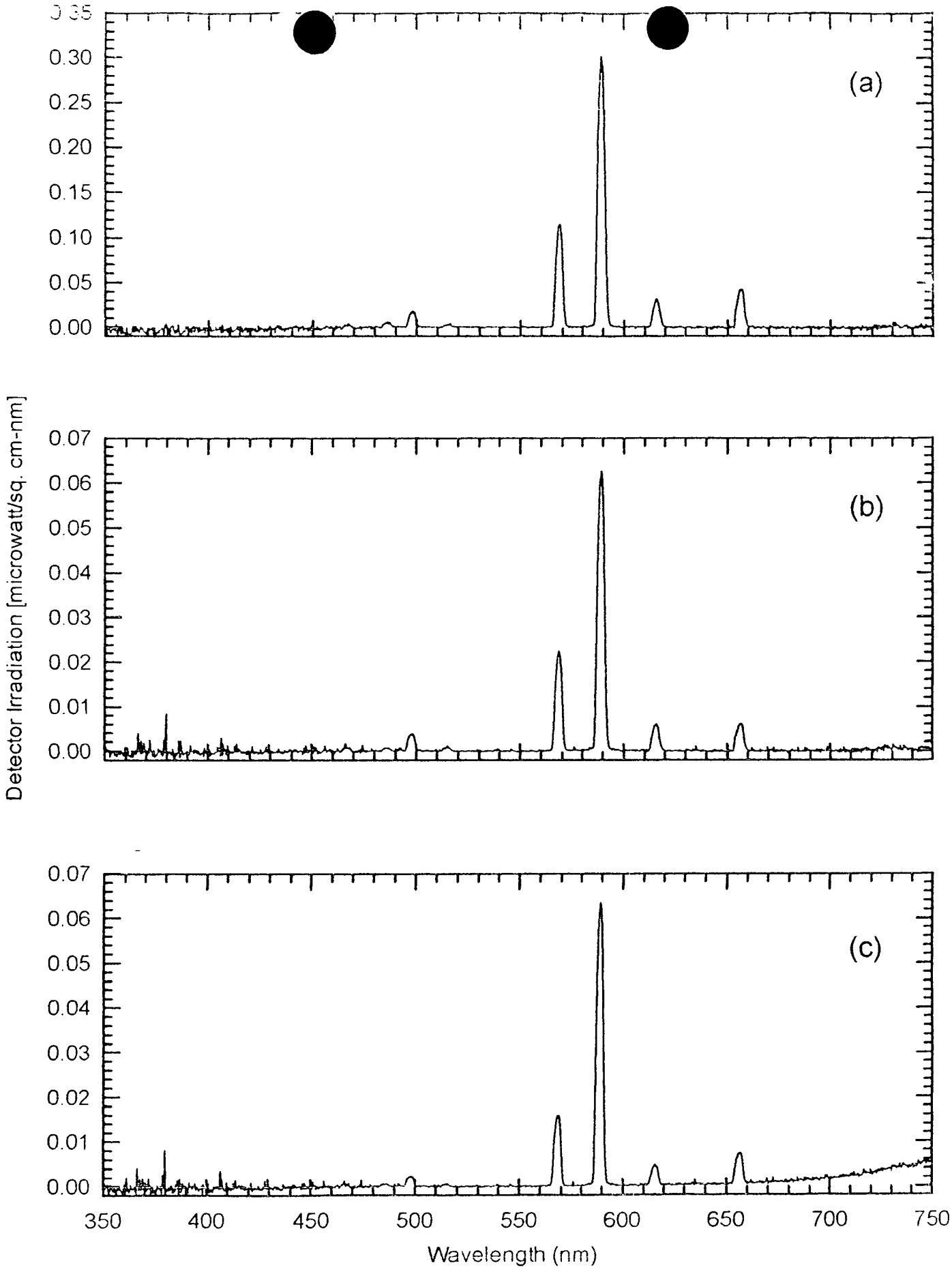
0.35
0.30
0.25
0.20
0.15
0.10
0.05
0.00
(a)
0.07
0.06
0.05
0.04
0.03
0.02
0.01
0.00
(b)
Detector Irradiation [microwatt/sq. cm-nm]
0.07
0.06
0.05
0.04
0.03
0.02
0.01
0.00
(c)
350
400
450
500
550
600
650
700
750
Wavelength (nm)

Fig. 23

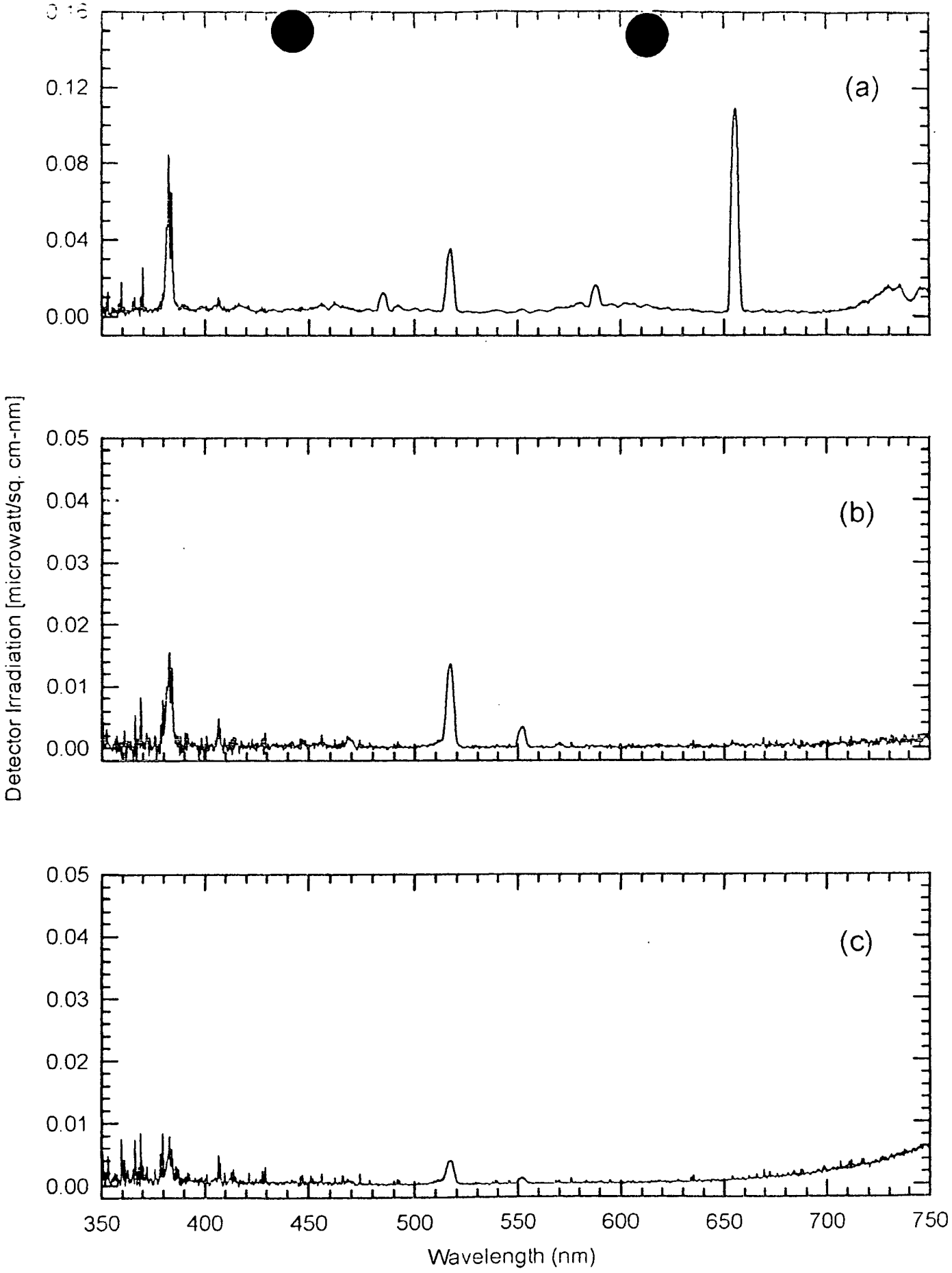
0.12
0.08
0.04
0.00
(a)
0.05
0.04
0.03
0.02
0.01
0.00
(b)
Detector Irradiation [microwatt/sq. cm-nm]
0.05
0.04
0.03
0.02
0.01
0.00
(c)
350
400
450
500
550
600
650
700
750
Wavelength (nm)

Fig. 24

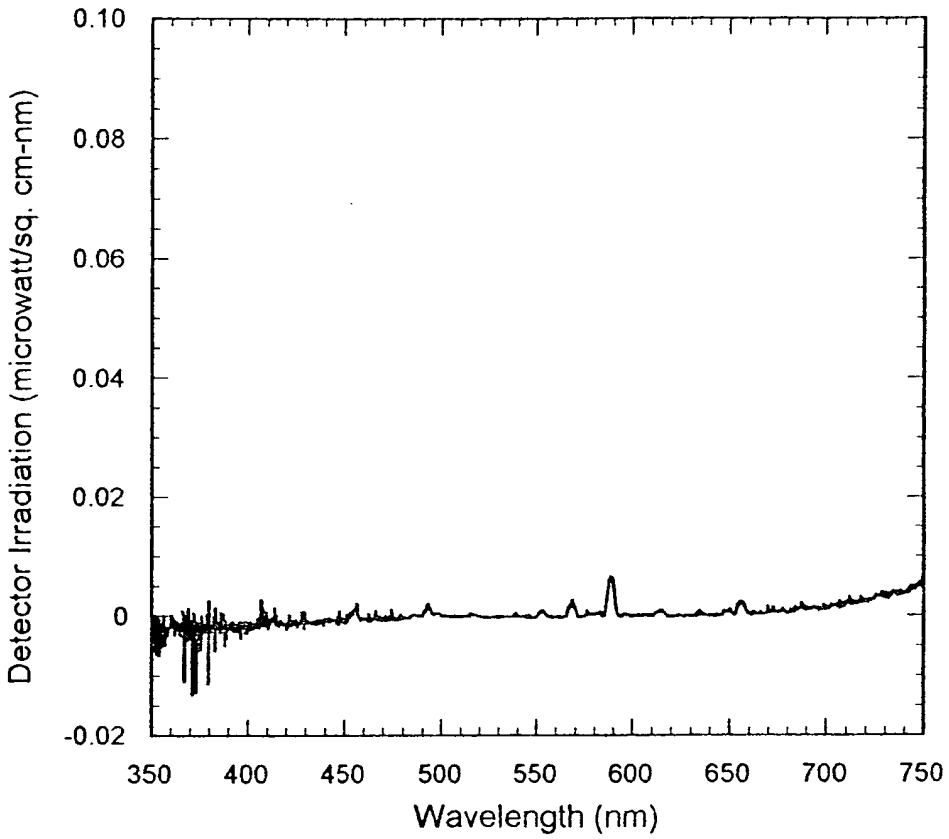
0.10
0.08
0.06
0.04
0.02
0
-0.02
Detector Irradiation (microwatt/sq. cm-nm)
350
400
450
500
550
600
650
700
750
Wavelength (nm)

Fig. 25

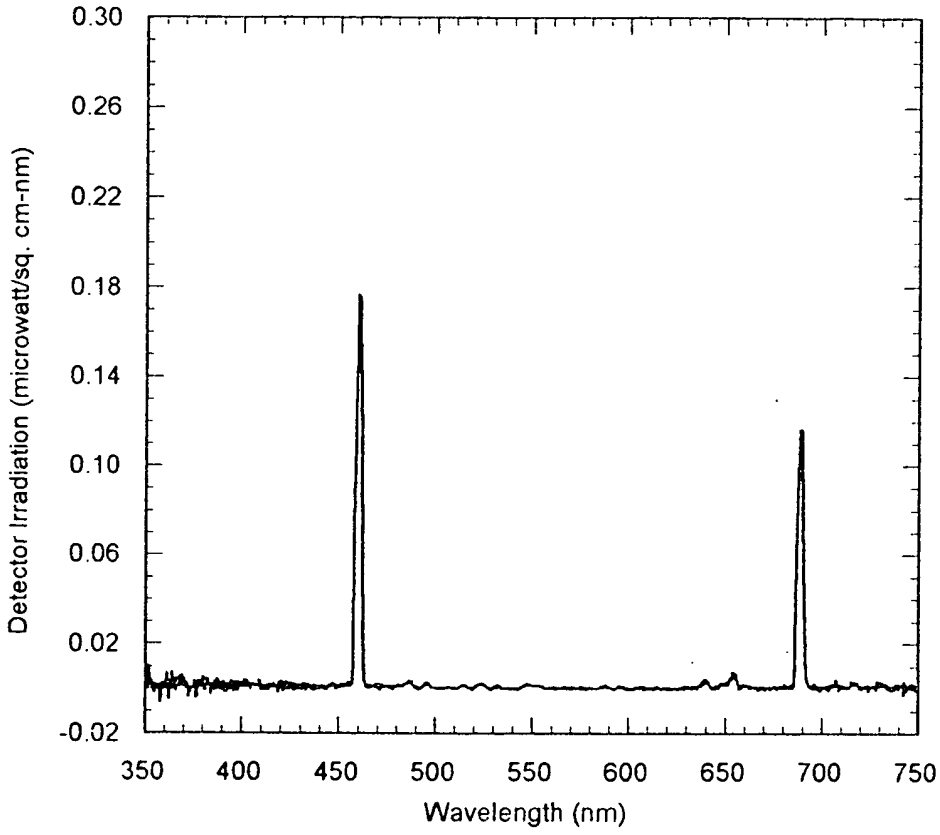
0.30
0.26
0.22
0.18
0.14
0.10
0.06
0.02
-0.02
Detector Irradiation (microwatt/sq. cm-nm)
350
400
450
500
550
600
650
700
750
Wavelength (nm)

Fig. 26

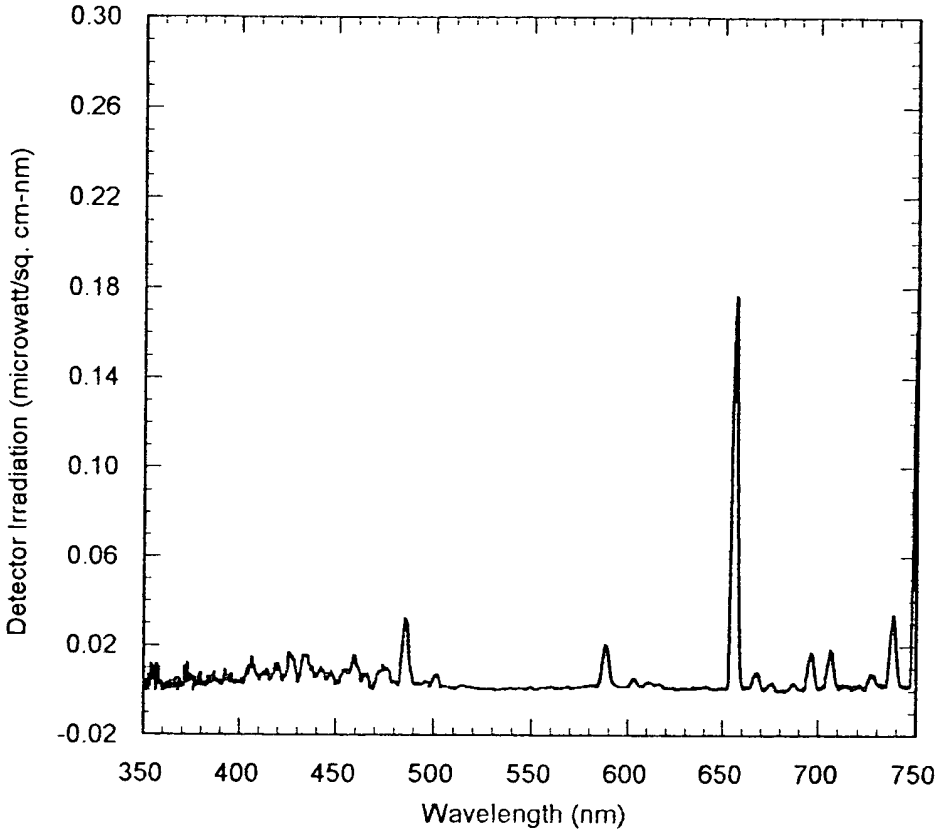
0.30
0.26
0.22
0.18
0.14
0.10
0.06
0.02
-0.02
Detector Irradiation (microwatt/sq. cm-nm)
350
400
450
500
550
600
650
700
750
Wavelength (nm)

Fig. 27

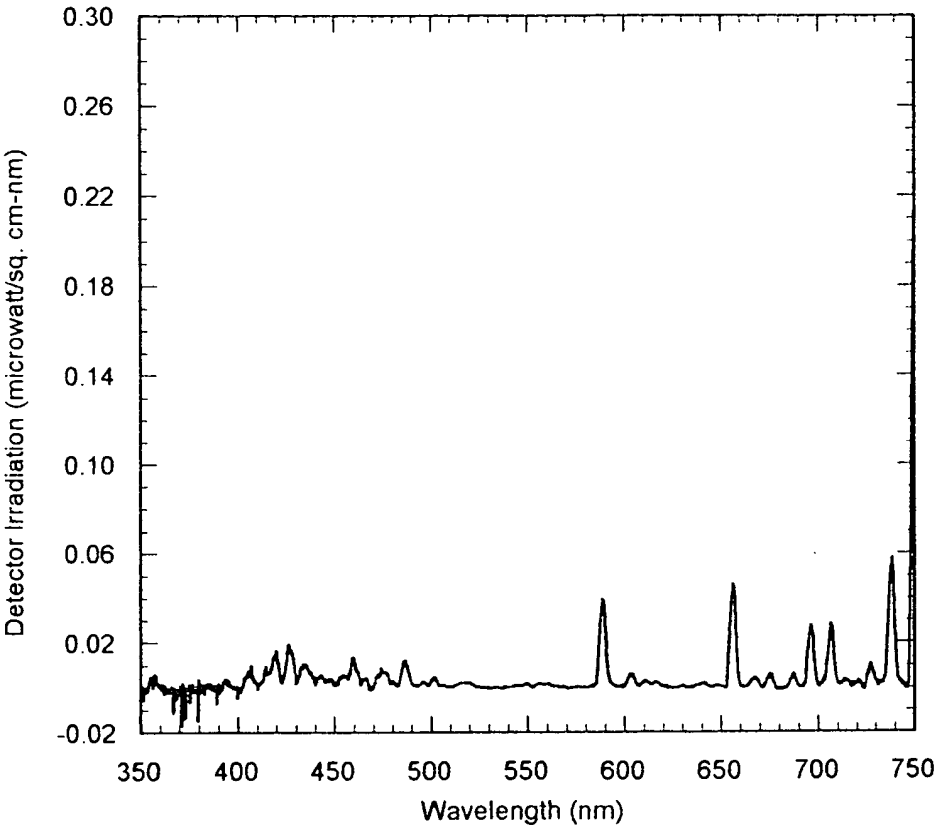
0.30
0.26
0.22
0.18
0.14
0.10
0.06
0.02
-0.02
Detector Irradiation (microwatt/sq. cm-nm)
350
400
450
500
550
600
650
700
750
Wavelength (nm)

Fig. 28